

RADC-TR-89-281
In-House Report
November 1989



RELIABILITY ASSESSMENT USING FINITE ELEMENT TECHNIQUES

Gretchen A. Bivens

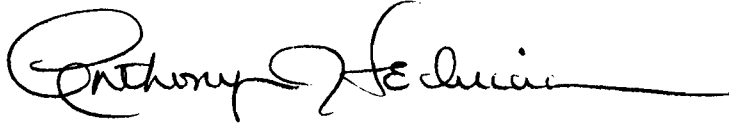
APPROVED FOR PUBLIC RELEASE; DISTRIBUTION UNLIMITED.

ROME AIR DEVELOPMENT CENTER
Air Force Systems Command
Griffiss Air Force Base, NY 13441-5700

This report has been reviewed by the RADC Public Affairs Office (PA) and is releasable to the National Technical Information Service (NTIS). At NTIS it will be releasable to the general public, including foreign nations.

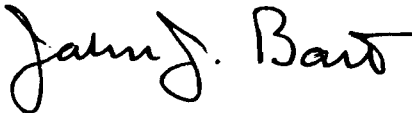
RADC TR-89-281 has been reviewed and is approved for publication.

APPROVED:



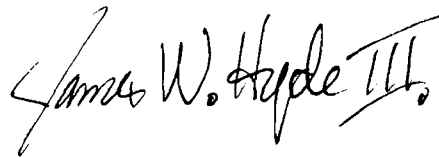
ANTHONY J FEDUCCIA
Chief, Reliability & Engineering Division
Directorate of Reliability and Compatibility

APPROVED:



JOHN J. BART
Technical Director
Directorate of Reliability and Compatibility

FOR THE COMMANDER:



JAMES W. HYDE III
Directorate of Plans and Programs

If your address has changed or if you wish to be removed from the RADC mailing list, or if the addressee is no longer employed by your organization, please notify RADC (RBES) Griffiss AFB NY 13441-5700. This will assist us in maintaining a current mailing list.

Do not return copies of this report unless contractual obligations or notices on a specific document requires that it be returned.

UNCLASSIFIED

SECURITY CLASSIFICATION OF THIS PAGE

REPORT DOCUMENTATION PAGE				Form Approved OMB No. 0704-0188		
1a. REPORT SECURITY CLASSIFICATION UNCLASSIFIED			1b. RESTRICTIVE MARKINGS N/A			
2a. SECURITY CLASSIFICATION AUTHORITY N/A			3. DISTRIBUTION / AVAILABILITY OF REPORT Approved for public release; distribution unlimited.			
2b. DECLASSIFICATION / DOWNGRADING SCHEDULE N/A						
4. PERFORMING ORGANIZATION REPORT NUMBER(S) RADC-TR-89-281			5. MONITORING ORGANIZATION REPORT NUMBER(S) N/A			
6a. NAME OF PERFORMING ORGANIZATION Rome Air Development Center		6b. OFFICE SYMBOL (If applicable) RBES	7a. NAME OF MONITORING ORGANIZATION Rome Air Development Center (RBES)			
6c. ADDRESS (City, State, and ZIP Code) Griffiss AFB NY 13441-5700			7b. ADDRESS (City, State, and ZIP Code) Griffiss AFB NY 13441-5700			
8a. NAME OF FUNDING / SPONSORING ORGANIZATION Rome Air Development Center		8b. OFFICE SYMBOL (If applicable) RBES	9. PROCUREMENT INSTRUMENT IDENTIFICATION NUMBER N/A			
8c. ADDRESS (City, State, and ZIP Code) Griffiss AFB NY 13441-5700			10. SOURCE OF FUNDING NUMBERS			
			PROGRAM ELEMENT NO. 62702F	PROJECT NO. 2338	TASK NO. 02	WORK UNIT ACCESSION NO. 2X
11. TITLE (Include Security Classification) RELIABILITY ASSESSMENT USING FINITE ELEMENT TECHNIQUES						
12. PERSONAL AUTHOR(S) Gretchen A. Bivens						
13a. TYPE OF REPORT In-House		13b. TIME COVERED FROM Jan 88 TO Jul 88		14. DATE OF REPORT (Year, Month, Day) November 1989		
15. PAGE COUNT 76						
16. SUPPLEMENTARY NOTATION N/A						
17. COSATI CODES			18. SUBJECT TERMS (Continue on reverse if necessary and identify by block number)			
FIELD	GROUP	SUB-GROUP				
14	04		Reliability			
20	13		Finite Element Analysis			
			Prediction Techniques			
			Material Failure			
19. ABSTRACT (Continue on reverse if necessary and identify by block number)						
<p>Finite element analysis (FEA) is a computer simulation technique that is used to predict the thermal and mechanical response of a structure. Rome Air Development Center (RADC) has used FEA to predict the response in various electronic assemblies. This particular study was concerned with the reliability of surface mounted microwire boards. A FEA of this assembly was simulated and the results used to estimate its useful life. This report gives a detailed account of the factors to be considered when performing a FEA and the procedure used to transfer the results to a reliability figure-of-merit.</p>						
20. DISTRIBUTION / AVAILABILITY OF ABSTRACT <input checked="" type="checkbox"/> UNCLASSIFIED/UNLIMITED <input type="checkbox"/> SAME AS RPT. <input type="checkbox"/> DTIC USERS			21. ABSTRACT SECURITY CLASSIFICATION UNCLASSIFIED			
22a. NAME OF RESPONSIBLE INDIVIDUAL GRETCHEN A. BIVENS			22b. TELEPHONE (Include Area Code) (315) 330-4891		22c. OFFICE SYMBOL RADC(RBES)	

DD Form 1473, JUN 86

Previous editions are obsolete.

SECURITY CLASSIFICATION OF THIS PAGE

UNCLASSIFIED

UNCLASSIFIED

UNCLASSIFIED

TABLE OF CONTENTS

Chapter	Title	Page
0.0	EXECUTIVE SUMMARY	1
1.0	INTRODUCTION	3
2.0	RELIABILITY CONCERNS IN ELECTRONIC ASSEMBLIES	5
3.0	STUDY METHOD	10
4.0	FINITE ELEMENT MODELING	20
4.1	MODELING OF COMPLIANT CONNECTIONS	21
4.1.1	SYSTEMS MODELS	21
4.1.2	BOARD MODEL	32
4.1.3	COMPLIANT CONNECTION MODELS	32
4.2	MODELING OF COMPLEX CIRCULAR GEOMETRIES	40
4.3	LESSONS LEARNED	46
5.0	TRANSFER OF FINITE ELEMENT RESULTS	48
5.1	S-LEAD CONNECTION	49
5.2	LEADLESS CONNECTION	52
5.3	GULL-WING CONNECTION	54
5.4	MICROWIRE/PTH CONNECTION	57
6.0	CONCLUSIONS	63
7.0	REFERENCES	66

LIST OF ILLUSTRATIONS

Figure	Title	Page
1	Four Surface Mounted Package Designs	6
2	Microwire Construction	7
3	Microwire Construction	8
4	Microwire Construction	8
5	3-D Solid Elements	11
6	Typical One-Quarter Geometry	12
7	Stress-Strain Curve for a Ductile Material	14
8	Bounded Plastic Region	15
9	Coffin-Manson Model	16
10	Coffin-Manson Curve for Copper	18
11	Coffin-Manson Curve for Solder	19
12	S-Lead System FEM Generation	23
13	S-Lead System Superelement Model	24
14	S-Lead System FEM	25
15	Leadless System FEM Generation	26
16	Leadless System Superelement Model	27
17	Leadless System FEM	28
18	Gull-Wing System FEM Generation	29
19	Gull-Wing System Superelement Model	30
20	Gull-Wing System FEM	31
21	Microwire Board FEM	32
22	S-Lead Superelement Model	33
23	S-Lead FEM	34
24	Solder Joint: X-Y Plane	35
25	Solder Joint: X-Z Plane	36
26	Solder Joint: Y-Z Plane	37
27	Leadless FEM	38
28	Gull-Wing Superelement Model	39
29	Gull-Wing FEM	39
30	Wire Within a Block	41
31	Meshed Block	41
32	Microwire/PTH FEM Generation	43

33	Microwire/PTH FEM	44
34	Modified Microwire/PTH FEM (20 Mil Via)	45
35	Modified Microwire/PTH FEM (10 Mil Via)	45
36	Stress Contours for S-Lead FEM	50
37	Stress Contours for Leadless FEM	53
38	Stress Contours for Gull-Wing FEM	55
39	Stress Contours for Microwire/PTH (20 Mil Via) FEM	58
40	Stress Contours for Microwire/PTH (10 Mil Via) FEM	59

0.0 EXECUTIVE SUMMARY

Finite element analyses (FEA) are increasingly being used to predict the mechanical response of an electronic assembly exposed to thermal and vibrational environments. The results of these analyses are used to estimate a component's life. This technique provides engineers with a method of assessing the reliability of emerging technologies associated with electronic systems. This particular investigation was concerned with the reliability of surface mounted solder interconnections and microwire board's plated-thru-hole (PTH) connections when exposed to severe thermal environments. These two interconnections were analyzed using FEA and an estimate of the number of cycles to failure was made.

There are many factors that must be considered before performing a finite element analysis. Are the materials relatively well known and the proper material properties available for this analysis? Are the boundary conditions, input conditions and environment of the system known? How complex is the geometry to be modeled? Can any assumptions be made to simplify the model? It is important that the engineer performing the analysis be aware of the information available in order to decide whether an analysis is feasible and if so, what the best approach to performing the study would be.

When modeling a new, complex system, preliminary modeling becomes important. Investing this initial effort reduces the overall analysis time and cost, and increases the results' accuracy. Examples of

preliminary modeling which were performed in this investigation are documented in the body of this report.

The results of the FEA were plotted on either the Coffin-Manson curve for copper or for solder, depending on the material being analyzed. The Coffin-Manson curve relates the material's strain to the number of cycles to failure. This cycles to failure value gives an estimation of the life of these connections. This method of transferring FEA results to an estimated life allows the design and reliability engineer to locate areas of reliability concern and make the corresponding corrections early in the program. This reduces the overall cost of the program and allows the reliability of the system to be built in. This technique is especially important for military systems incorporating new technologies.

1.0 INTRODUCTION

RADC has used finite element analysis (FEA) as a way to assess the reliability of emerging technologies. In the past, the resulting stress values were taken from the FEA results and compared with the strength of the corresponding materials. It was soon realized, however, that a technique was needed to transfer the numerical results from the FEA to a measure of useful life for the system being analyzed. This report documents a reliability assessment of the areas of reliability concern in electronic assemblies through the use of FEA and a transfer of FEA results to an estimation of the useful life for the areas of concern.

Two areas of reliability concern were identified for the electronic assembly analyzed. The first area was the solder connection between a surface mounted device and its connecting board. Current use of these devices has shown that these connections tend to fail soon after the system has been installed. Three different lead designs were evaluated, the S-lead, leadless, and gull-wing designs. The second area of concern was the interface connection between the microwire and the PTH. Microwire layering is a new technology that is being used to replace conventional signal layers in a surface mounted board. The connection with the PTH is critical to the use of microwire technology.

Once the areas of reliability concern are identified, the evaluation engineer determines the best way to develop the finite element model. A geometric model representing the physical system is generated and a data

file which describes the materials used, the boundary conditions, and the input conditions is created. This data file is read by the finite element simulation code and a thermal analysis performed. From this analysis, the strain range for the material of concern is obtained. Once the strain range in a monotonic thermal cycle is known, theoretical relations are used to estimate the number of thermal cycles this material would survive before failure.

2.0 RELIABILITY CONCERNS IN ELECTRONIC ASSEMBLIES

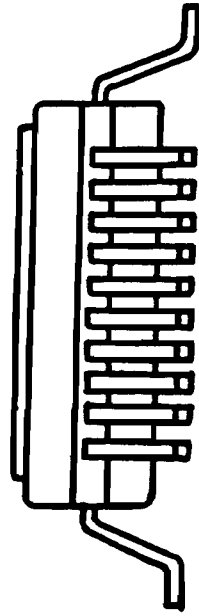
As technology has advanced and electronic assemblies become more complex, there is an increasing concern pertaining to the reliability of these systems. A highly specialized system that cannot perform its function is useless to the overall system. This is very critical when the system is a military aircraft or spacecraft. However, in order to implement many of the emerging technologies, unique packaging designs must be developed. If these unique designs are analyzed in the initial phase of a program, considerable time and money are saved.

The military was concerned with the reliability of surface mounted multilayer assemblies investigated in this study. These boards are using new mounting techniques and large packaging densities which have led to problems in the reliability of the interconnects. In particular, the failure of the leads of the surface mounted components is currently a driving failure mechanism in the reliability of these boards. Figure 1 shows typical surface mounted packages for four different lead designs. Factors which have been shown to effect the solder connection failure include the lead design, package size, board material and heat removal.

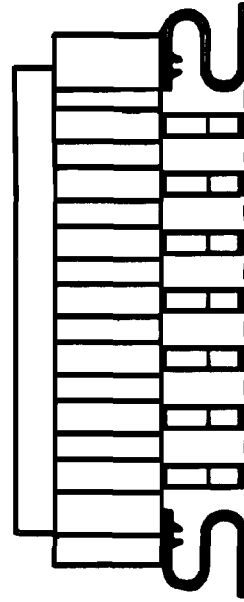
In order to minimize the solder connection failure mode, board materials which reduce the board's horizontal expansion were used. This reduction has caused an increase in the board's vertical expansion which has led to an increase in PTH connection failures. This assembly used microwire



LEADLESS CHIP CARRIER



"GULL-WING" LEADED CHIP CARRIER



S-LEAD CHIP CARRIER



"J" LEADED CHIP CARRIER

Figure 1: Four Surface Mounted Package Designs

boards which have a reduced vertical height of the board and thus a reduction in the overall vertical expansion of the board. There is a reliability concern, however, with the expansion that occurs at the microwire/PTH connection interface.

Microwires are insulated copper wires which are ultrasonically bonded to a dimensionally stable core (Figure 2). These wires are then encapsulated in a resin to form the microwire boards. PTHs, known as vias, are then laser drilled and the insulating material and encapsulating resin surrounding the copper wire is evaporated (Figure 3). The hole is then plated with copper and the interconnect between the PTH and the microwire is formed (Figure 4). This interconnect region is the second area of reliability concern.

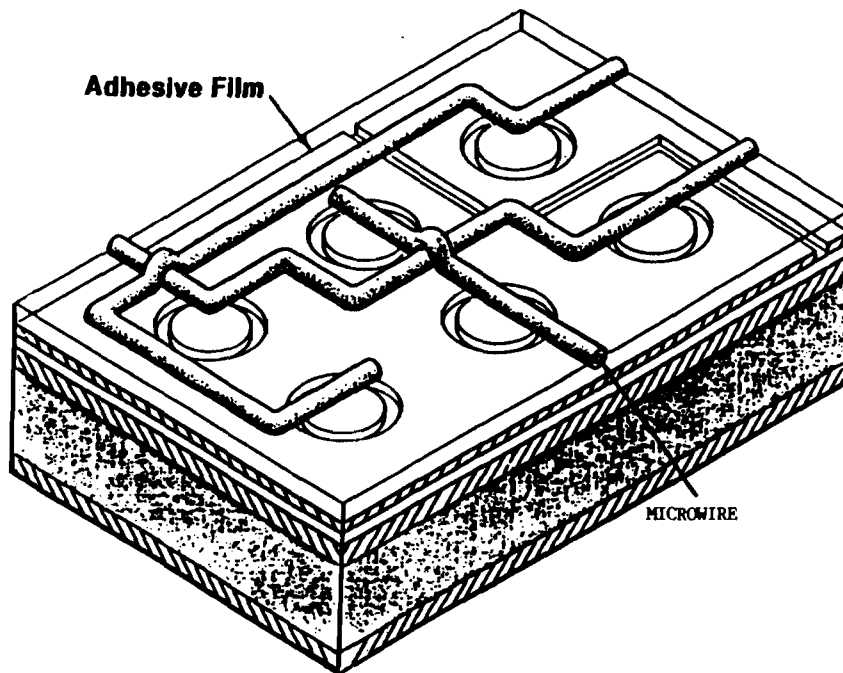


Figure 2: Microwire Construction

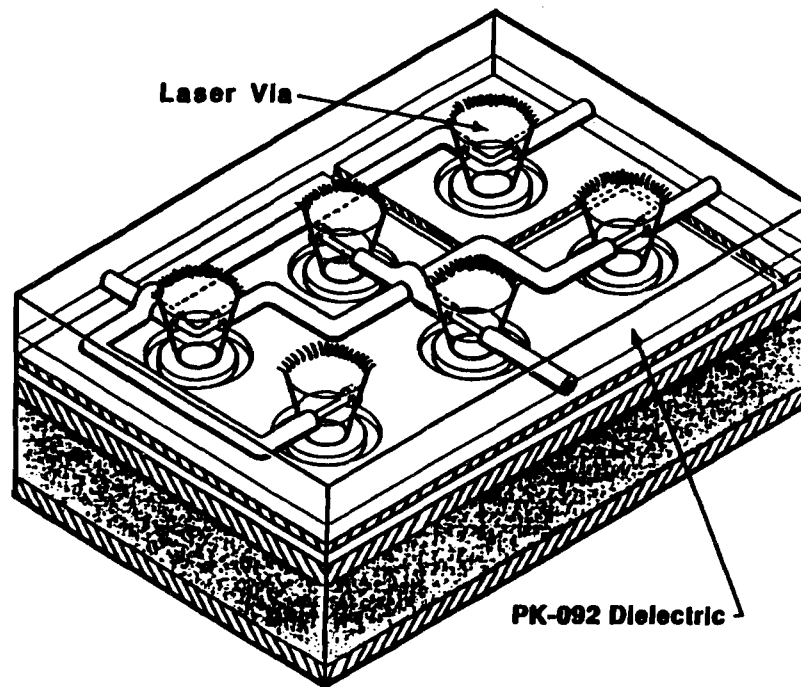


Figure 3: Microwire Construction

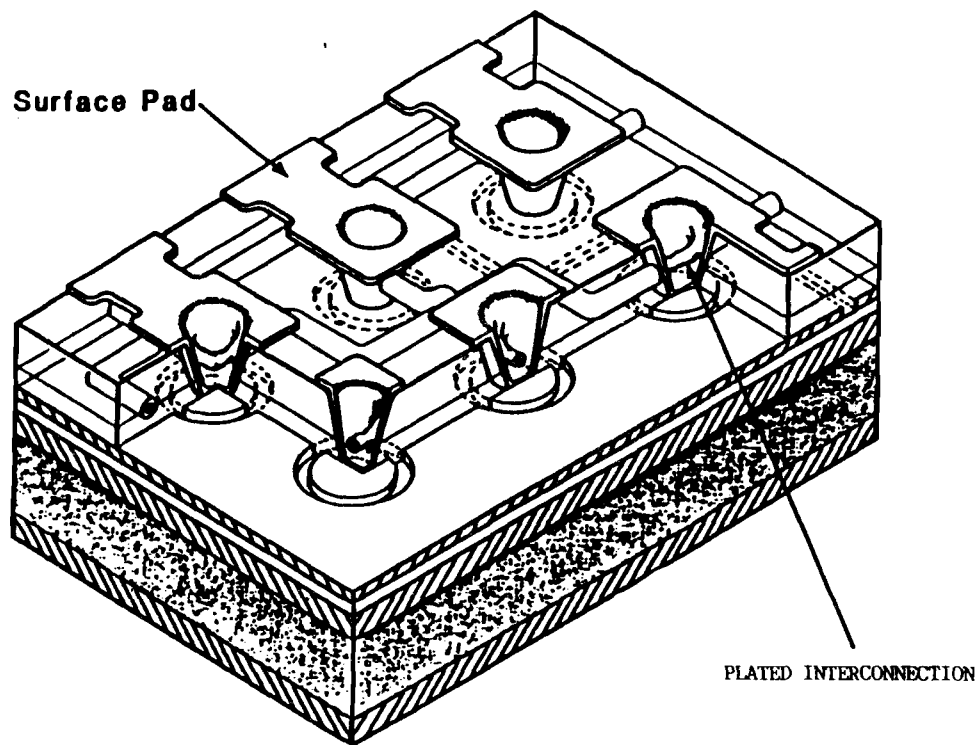


Figure 4: Microwire Construction

Before these interconnect problems became so prevalent, the Air Force assumed that adequate heat transfer and low package thermal resistance values guaranteed reliable assemblies. Studies at RADC, other DoD organizations and contractors have shown that this is not sufficient criteria for surface mounted assemblies due to the interconnect failure mode. The overriding problem with the reliability of interconnects is cyclic fatigue; that is, as these devices and connecting boards expand and contract, the interconnects between them are forced to expand and contract as well. Since these interconnects have become extremely small in size, it does not take very much expansion to cause a significant amount of strain to occur. Once the device and board return to the original state, so does the interconnect. A problem occurs because the materials used in these interconnects, solder and copper, tend to fail rapidly even when exposed to small amounts of cyclic strains.

3.0 STUDY METHOD

FEA is the technique currently used at RADC to evaluate the reliability of new microcircuit packaging designs. Over the past five years, RADC has used FEA to perform reliability evaluations on VHSIC, gallium arsenide, wafer scale integration, and surface mounted devices. The findings in these evaluations have had excellent correlation with the results from laboratory testing and field demonstration. Furthermore, FEA is increasingly being used in industry and other DoD organizations to design and evaluate microcircuit packages.

The FEA code that is used at RADC is Numerically Integrated Elements for System Analysis (NISA). NISA was developed by Engineering Mechanics Research Corporation, Troy MI. This program is used to perform a wide range of analyses including static stress, dynamic, buckling and heat transfer. In this study, NISA's static stress module was utilized to simulate the response of the surface mounted boards to varying temperature conditions.

In order to predict the physical response of the surface mounted microwire boards, finite element models (FEMs) were generated and a temperature change was simulated. FEMs are geometrical models which represent the actual physical system. The FEM is defined by two physical parameters, nodes and elements.

A node is a grid point located in space. In this study, the models were created in three dimensions and, therefore, each node was defined by three coordinates, (x, y, z) . The second parameter, the element, is defined by a material index number and a set of nodes. Each index number has specific material properties associated with it. The properties can be defined to be constant or to vary with temperature. Two of the materials used in this analysis had temperature-dependent properties and an equation relating the material property versus a temperature change was assigned to the material index number corresponding to those materials. The elements used in this study were three-dimensional (3-D), six-sided, solid elements. Two types of 3-D elements were utilized (Figure 5). The first type was identified by eight corner nodes. These elements are usually rectangular in shape, but do not have to be. This type of element uses linear equations to define the lines connecting the nodes. The second type of element is defined by eight corner nodes and twelve midside nodes. This type uses parabolic equations to define the lines connecting the nodes. This allows curved surfaces to be accurately modeled. Using 20 noded elements significantly increases the complexity of the model and the simulation.

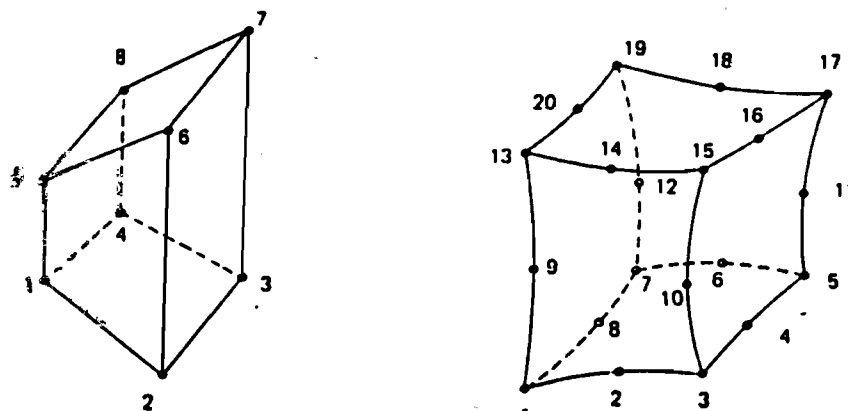


Figure 5: 3-D Solid Elements

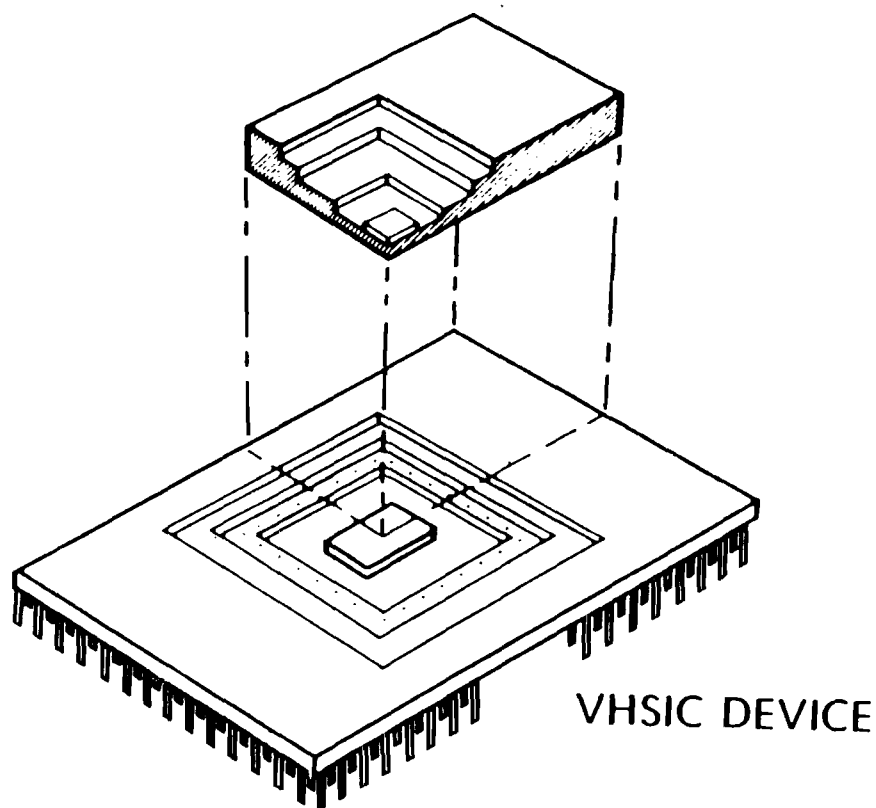


Figure 6: Typical One-Quarter Geometry

It is important when designing a FEM to keep its complexity to a minimum. One common way of reducing the model's complexity is to take advantage of the physical device's symmetrical geometry and boundary conditions. The FEMs developed in this study represent one quarter of the actual assembly. The boundaries at these symmetrical "cut" surfaces had to be constrained in the direction perpendicular to these surfaces. This prevented movement into the missing quarters. An example of a one-quarter geometry is displayed in Figure 6.

When choosing the temperature cycling range, many factors were considered. The most important was the environment that the microwire assemblies were experiencing in the field. The second was the temperature at which the assemblies are manufactured. This value was considered the stress free temperature of the assembly. All of the models were cycled twice, once from the stress free temperature to the maximum temperature (high temperature cycle) and once from the stress free temperature to the minimum temperature (low temperature cycle). The output strain from each of these analyses were added together to obtain the material's total strain.

When calculating the total strain in an analysis, the following procedure is used. First, the maximum Von-Mises stress in the ductile material (copper or solder) is tabulated. The Von-Mises stress value is a combined stress value used when predicting failure. If this stress is greater than the yield stress, then the elastic strain and the plastic strain must both be calculated. A typical stress/strain curve for a ductile material is shown in Figure 7. The strain in the elastic region is the elastic stress divided by the modulus of elasticity. The strain in the plastic region is then estimated using two different approaches. One approach underestimates the plastic strain, the other approach overestimates the strain and the actual strain is assumed to be in between these two values. Figure 8 shows how the first approach estimates the plastic strain by extending the straight stress/strain line from the elastic region into the plastic region. The second approach takes twice the

plastic strain that is estimated in the first approach and adds this to the elastic strain, thus giving the lower bound of the region.

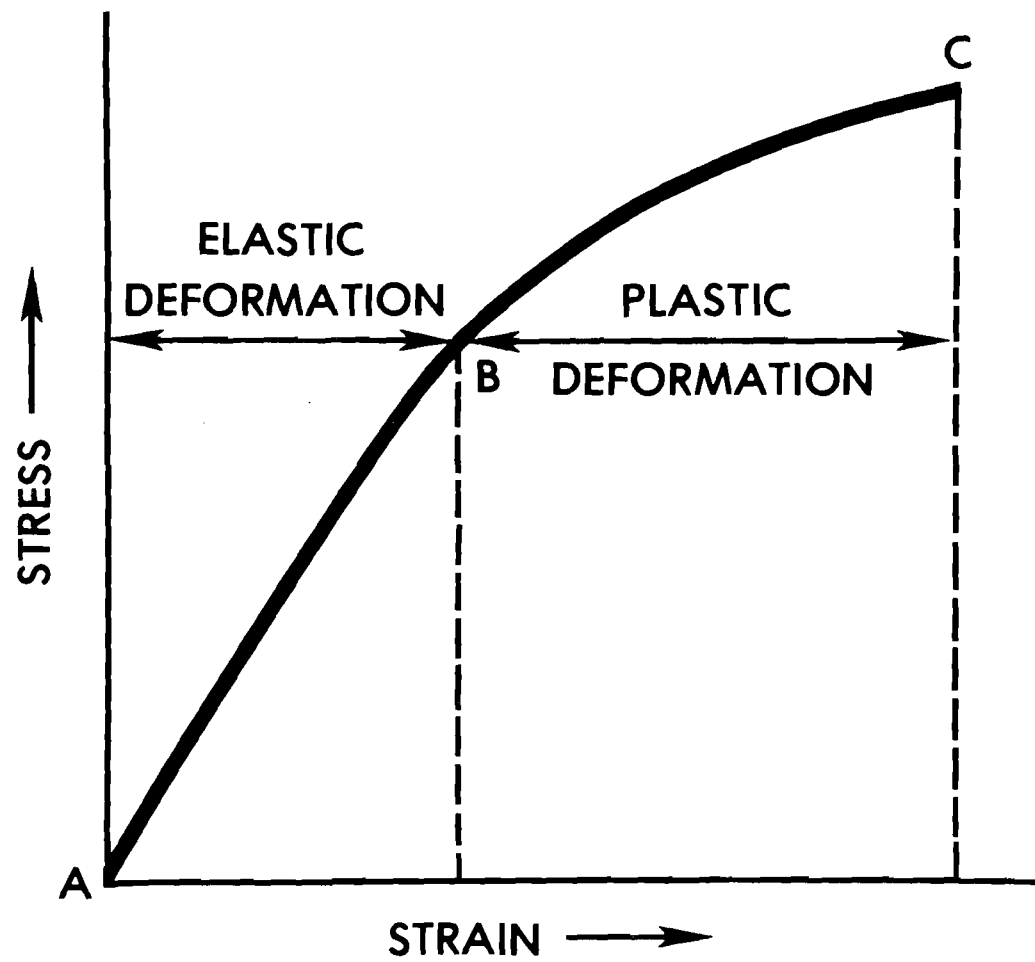


Figure 7: Stress-Strain Curve For A Ductile Material

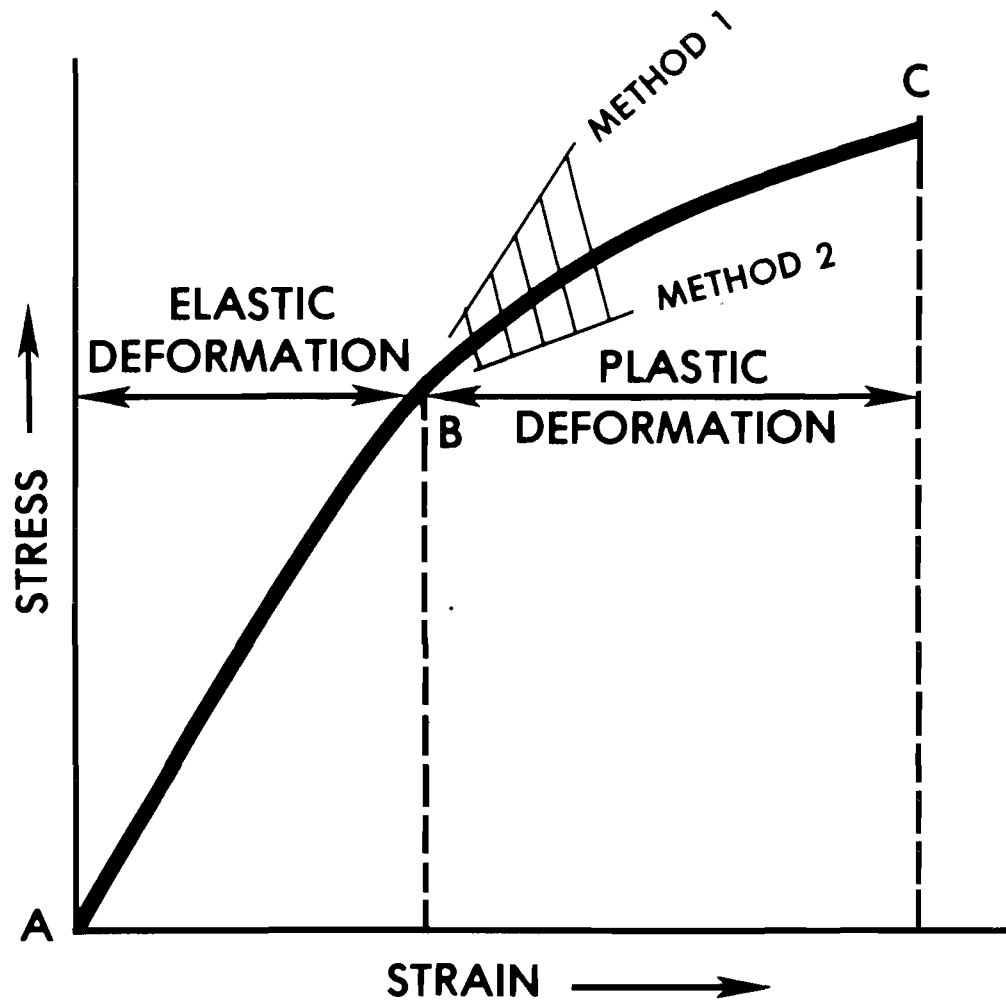


Figure 8: Bounded Plastic Region

The total strain is calculated by adding the elastic and plastic strains for the two temperature cycles. This total strain value is transferred into a number of cycles to failure value using the Coffin-Manson Curve for the specific material. This curve is generated from the Coffin-Manson model displayed in Figure 9. In order to use this formula, the coefficients associated with the material of interest must be known. The

$$\frac{\Delta \epsilon}{2} = \underbrace{\frac{\sigma_f}{E} (2N_f)^b}_{\text{ELASTIC STRAIN}} + \underbrace{\epsilon_f (2N_f)^c}_{\text{PLASTIC STRAIN}}$$

<u>PARAMETER</u>	<u>COPPER</u>	<u>SOLDER</u>
σ_f	50,050 psi	7,350 psi
ϵ_f	.3	.325
E	16×10^6 psi	1.09×10^6 psi
b	-.05	-.05
c	-.6	-.5

σ_f : FATIGUE STRENGTH COEFFICIENT

ϵ_f : FATIGUE DUCTILITY COEFFICIENT

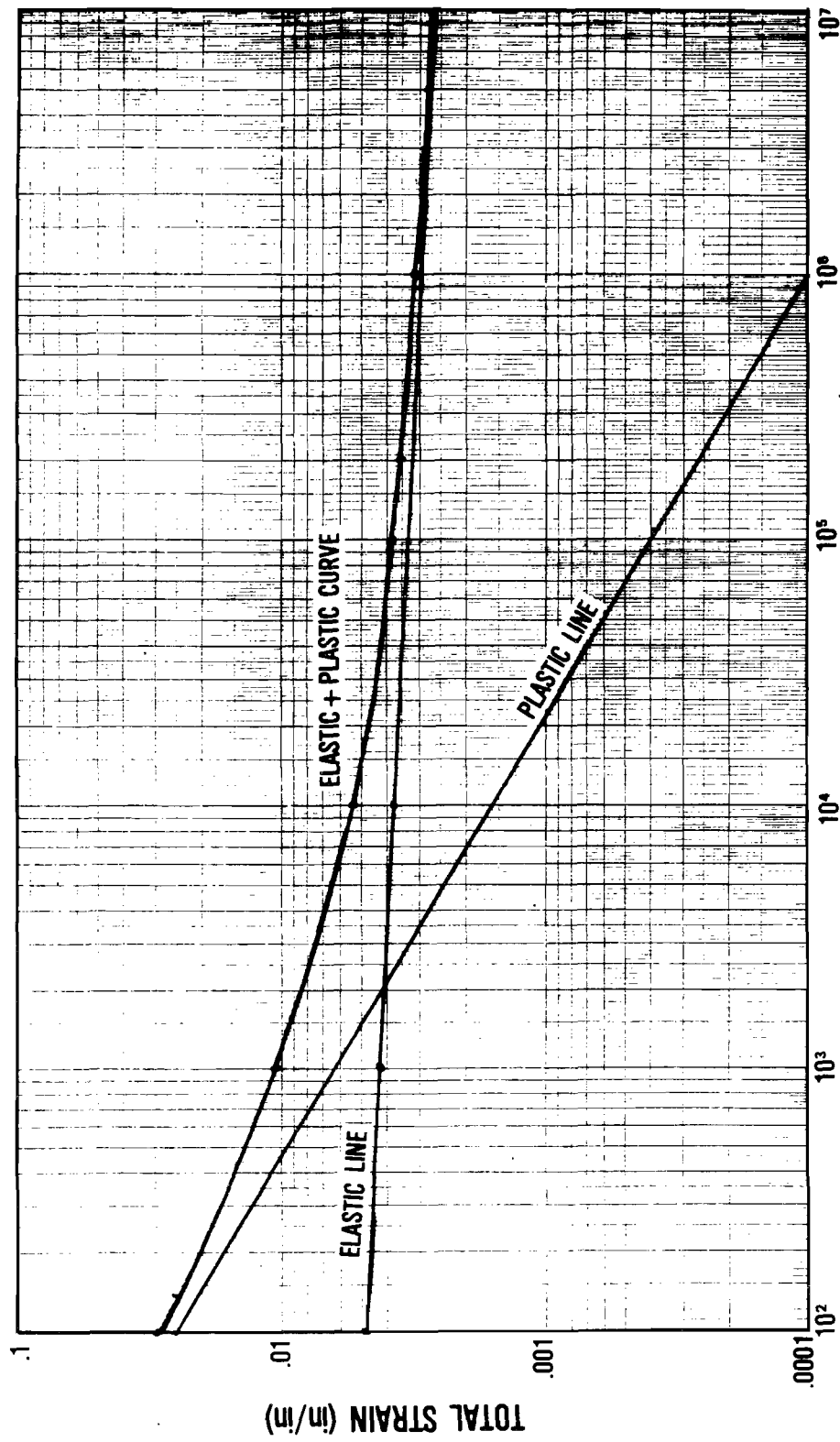
E : MODULUS OF ELASTICITY

b : FATIGUE STRENGTH EXPONENT

c : FATIGUE DUCTILITY EXPONENT

Figure 9: Coffin-Manson Model

values for the copper and solder are listed in Figure 9. These values were inserted into the model and the corresponding curves were generated, Figures 10 and 11. Each figure has two lines and one curve. The lines represent the elastic strain component and the plastic strain component and the curve represents the combined strain. In order to determine the number of cycles to failure for a given strain, the total strain value for this copper or solder is plotted onto the corresponding curve and the number of cycles to failure value is extrapolated.



NUMBER OF CYCLES TO FAILURE

Figure 10: Coffin-Manson Curve for Copper

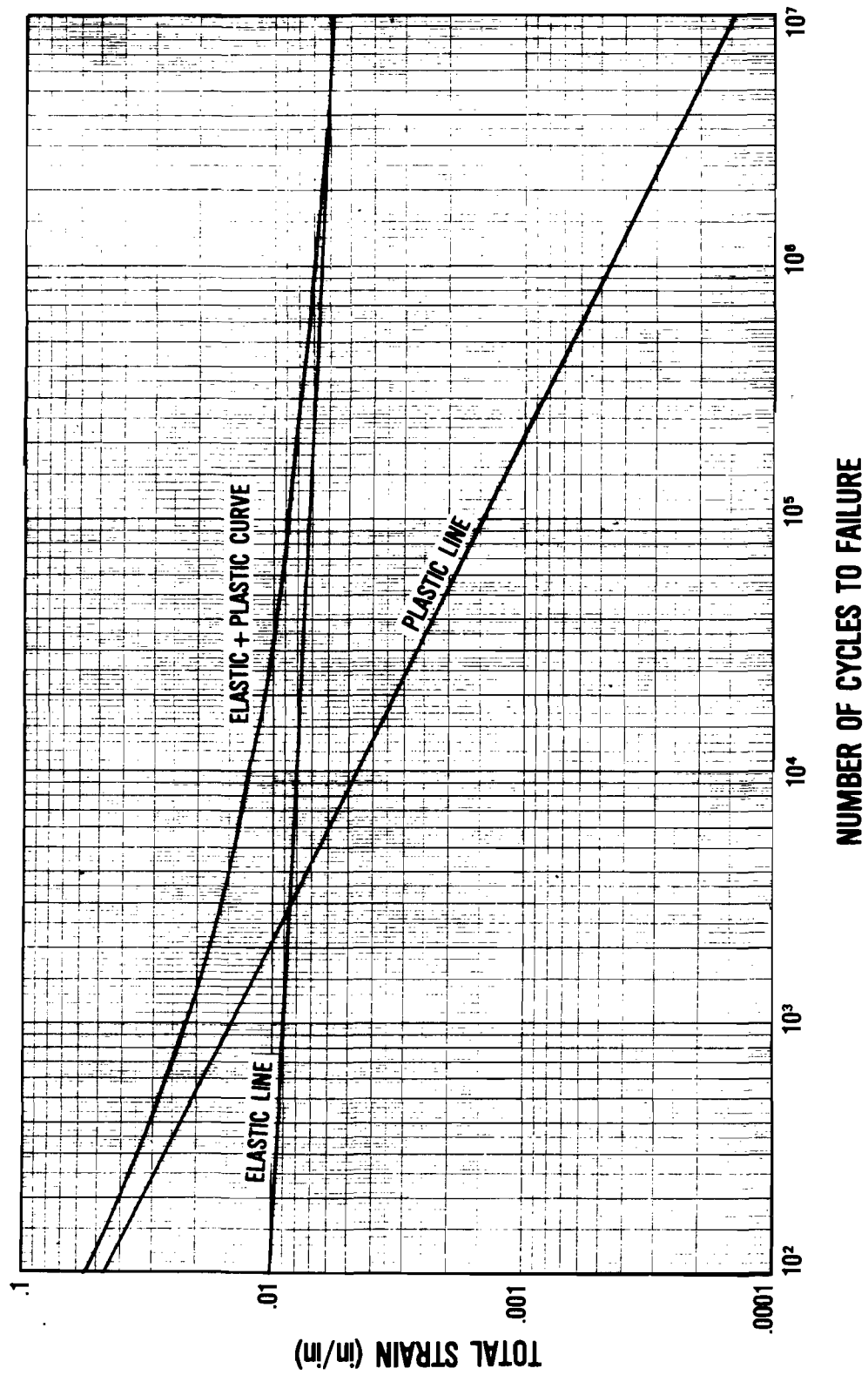


Figure 11: Coffin-Manson Curve for Solder

4.0 FINITE ELEMENT MODELING

When the engineer performing the FEA has an extensive knowledge in the area being analyzed, assumptions about the geometry, materials, and boundary and input conditions can be made. This is not always the case. An engineer may be given the basic information and asked to investigate the reliability of the system. Engineering judgment can be used to form some assumptions and other assumptions can be made as a result of preliminary modeling. Preliminary modeling is very important because incorrect assumptions can have a significant effect on the results of the analysis. These models are simple and are analyzed in a short time period compared to the overall time of the analysis. If the preliminary models result in assumptions that simplify the model, the time spent performing the analysis is reduced. Since most systems are too complex to be modeled in exact detail, assumptions have to be made so that the analysis can be performed in a timely manner.

Another reason preliminary modeling is useful is in reducing the chances of round-off error when modeling complex geometries. Round-off errors can result from several different factors including elements that are too large, are improperly formed, and have unusual geometries. Simple models representing the general shape of the complex geometry can indicate to the engineer whether the model's basic design will have problems before the more complex model is developed. The finite element model of the microwire and PTH connection interface is an example of this.

4.1 MODELING OF COMPLIANT CONNECTIONS

Three different compliant connections were modeled using the same general procedure. A model representing the package, board, and connection system was modeled. This is referred to as the system model. The deflections resulting from a thermal analysis of this model were then inputted into a model representing the compliant connection. Because the system has symmetrical geometries and boundary conditions, only one quarter of the system was modeled. The compliant connection did not have symmetrical boundary conditions, therefore, the entire connection was modeled.

During the generation of the system model, it became apparent that the model had too many elements for RADCS's computer capabilities. To reduce the large number of elements, the eight layers of microwire board were represented by a separate model and the resulting deflections inputted into the system model. Only the top layer of the microwire board was represented in the system model. Once both analyses were simulated, a comparison was made between the deflections along the top surface of the board for the board-alone model and for the system model. The results showed that the differences in the deflections were negligible and, therefore, this procedure was accurate.

4.1.1 SYSTEM MODELS

When generating a system finite element model, the following procedure was used. The figures given will represent the generation of the S-

lead system model. The S-lead package was a .45 x .55 inch package with 32 leads. First, a two-dimensional drawing representing a segment of the package and board and the S-lead was generated (Figure 12a). This model was then extended in the third dimension (Figure 12b). Now a second two-dimensional set of elements was created in a direction perpendicular to the first set. This set represented the same configuration as the first set and the nodes along the left side were taken from the original set of elements (Figure 12c). This second set of elements was then extended in the third dimension in the direction opposite to the first set of elements (Figure 12d). Now two sets of three-dimensional elements existed. These sets of elements were defined with different orientations and, therefore, the second set of elements was redefined to conform with the first set of elements.

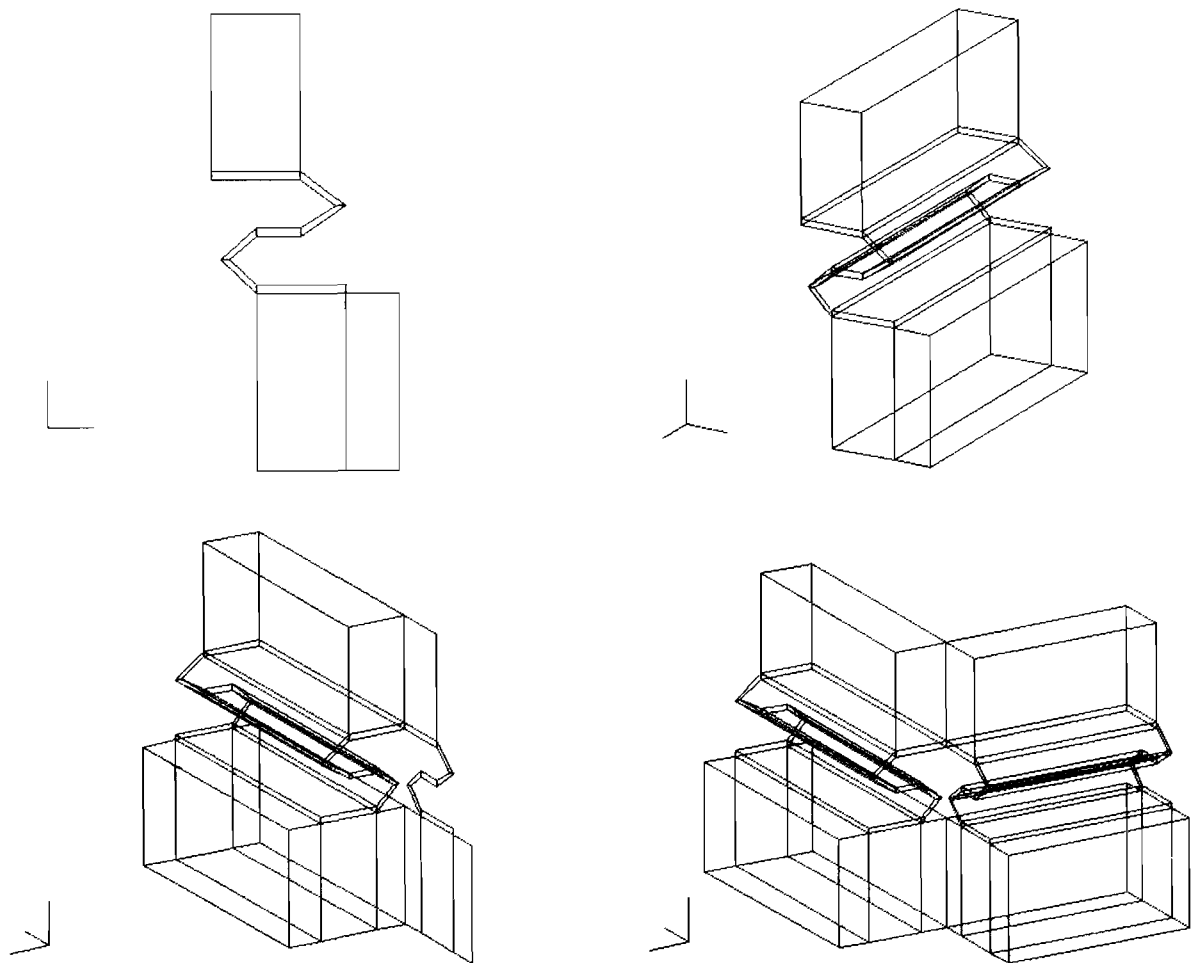


Figure 12: S-Lead System FEM Generation

The remaining package and board elements were generated (Figure 13), thus completing the superelement model. Because there was a small number of leads, the overall model was meshed so that the node points corresponded to the location of the leads. The elements representing the air spaces in between the leads were then deleted. The final finite element model is shown in Figure 14. The proper boundary conditions and temperature conditions were inputted into the data file and the analysis executed.

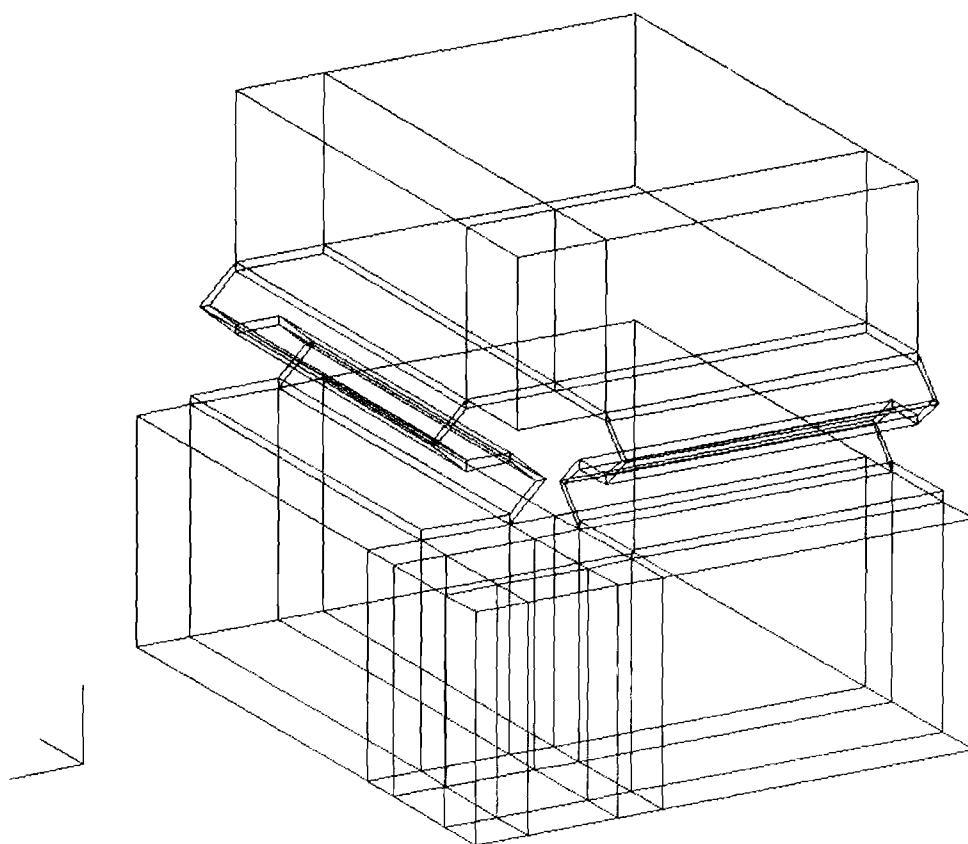


Figure 13: S-Lead System Superelement Model

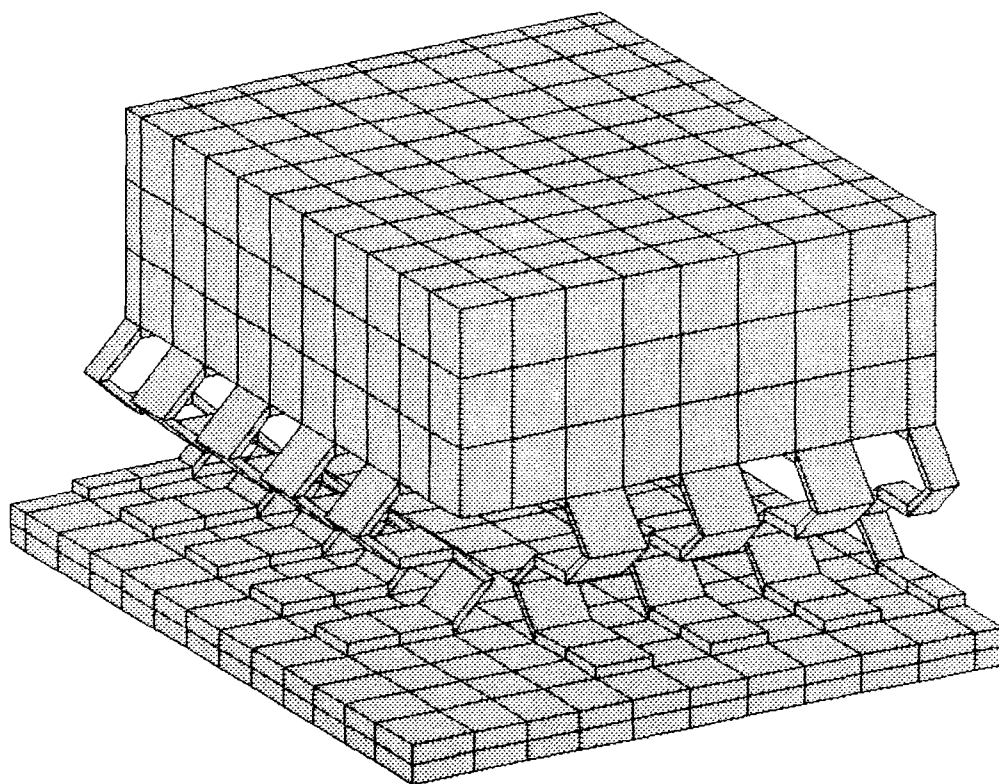
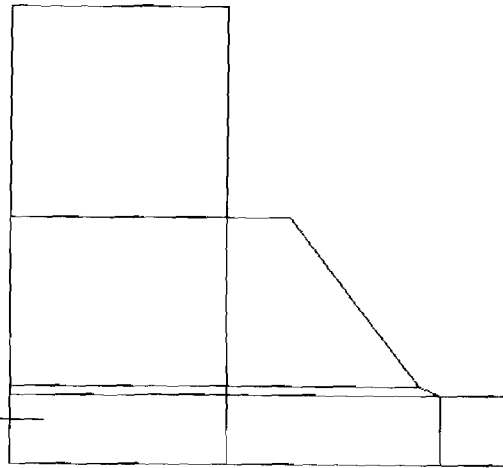
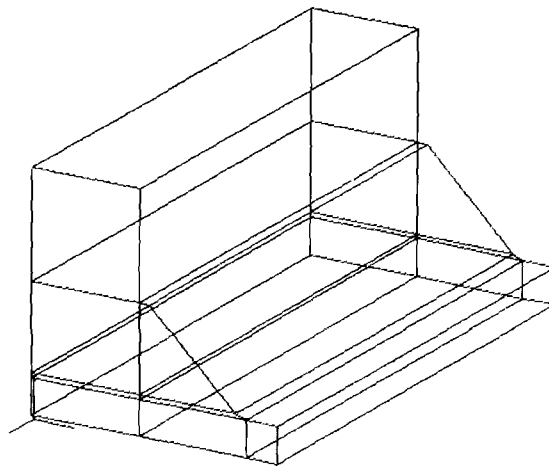


Figure 14: S-Lead System FEM

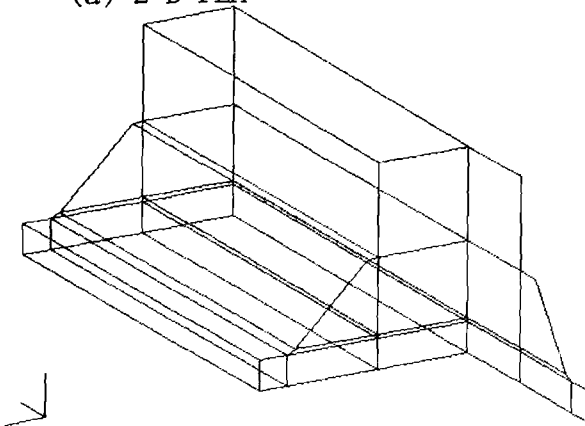
Since the leadless chip carrier (LCC) was also a .45 x .55 inch package with 32 connections, the same procedure was used to generate the system model for the LCC as shown in Figures 15, 16, and 17. The gull-wing package was a .94 x .94 inch package with 172 leads. The superelement model was generated using the same procedure as used for the S-lead system.



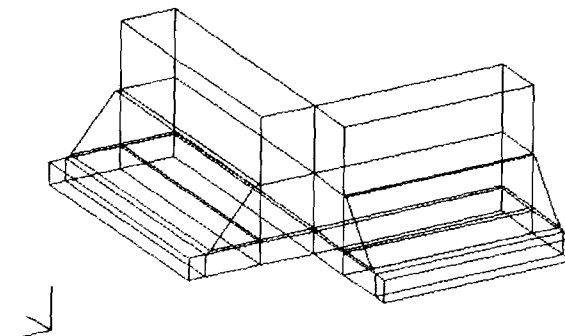
(a) 2-D FEM



(b) 3-D FEM



(c) Additional 2-D FEM



(d) Additional 3-D FEM

Figure 15: Leadless System FEM Generation

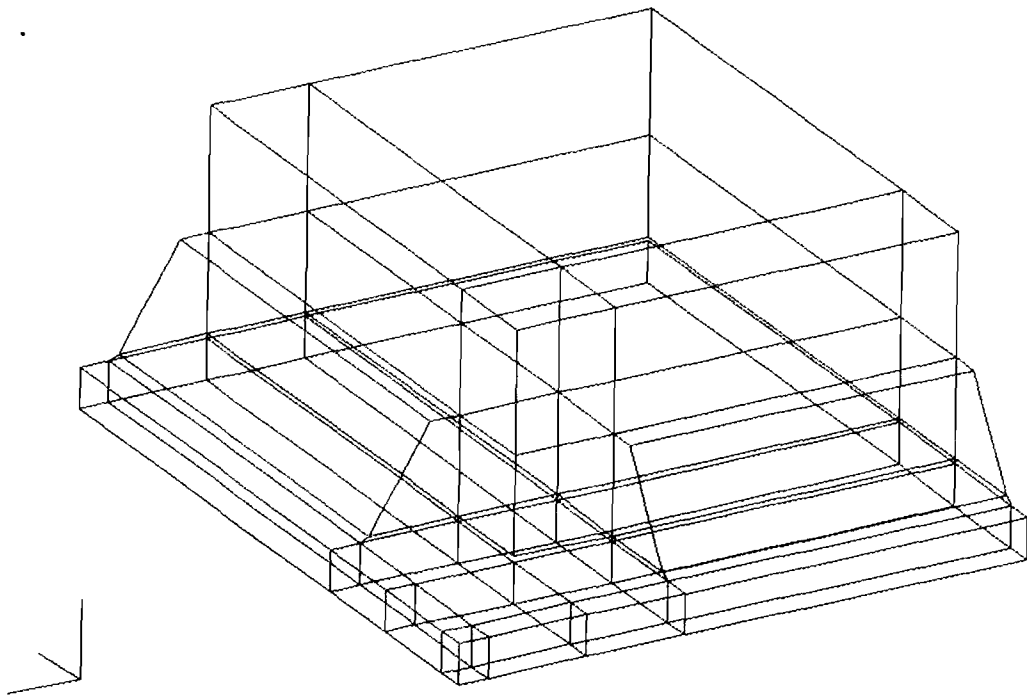


Figure 16: Leadless System Superelement Model

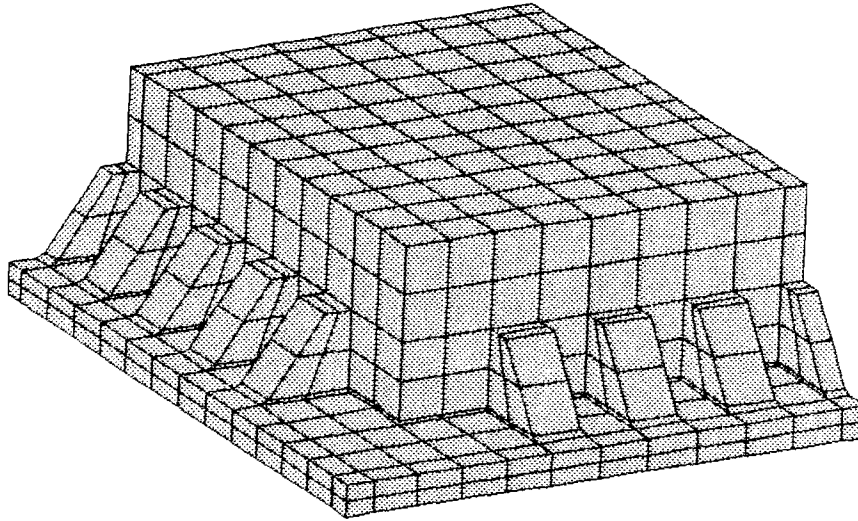
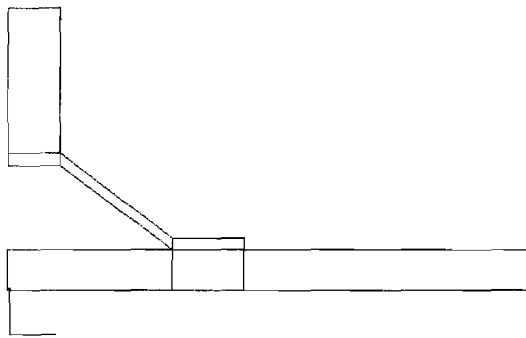
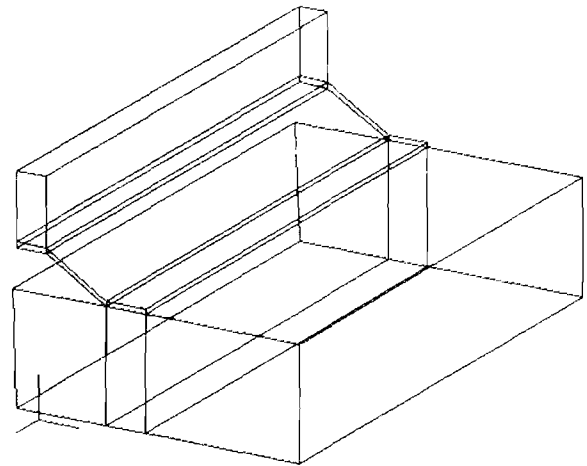


Figure 17: Leadless System FEM

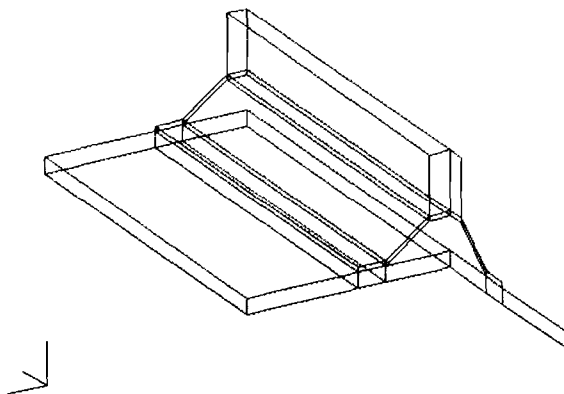
Due to the large package size and the large number of leads, the model could not be meshed so that the node points would correspond to the location of the leads. Therefore, the final model had approximately the same meshing configuration as the other models and the material properties of the solder and air materials were combined to give a set of equivalent properties. The gull-wing system model is represented in Figures 18, 19, and 20.



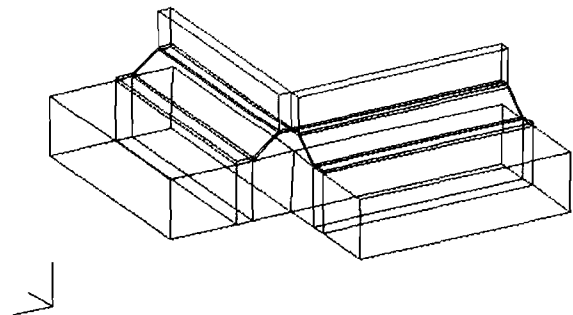
(a) 2-D FEM



(b) 3-D FEM



(c) Additional 2-D FEM



(d) Additional 3-D FEM

Figure 18: Gull-Wing System FEM Generation

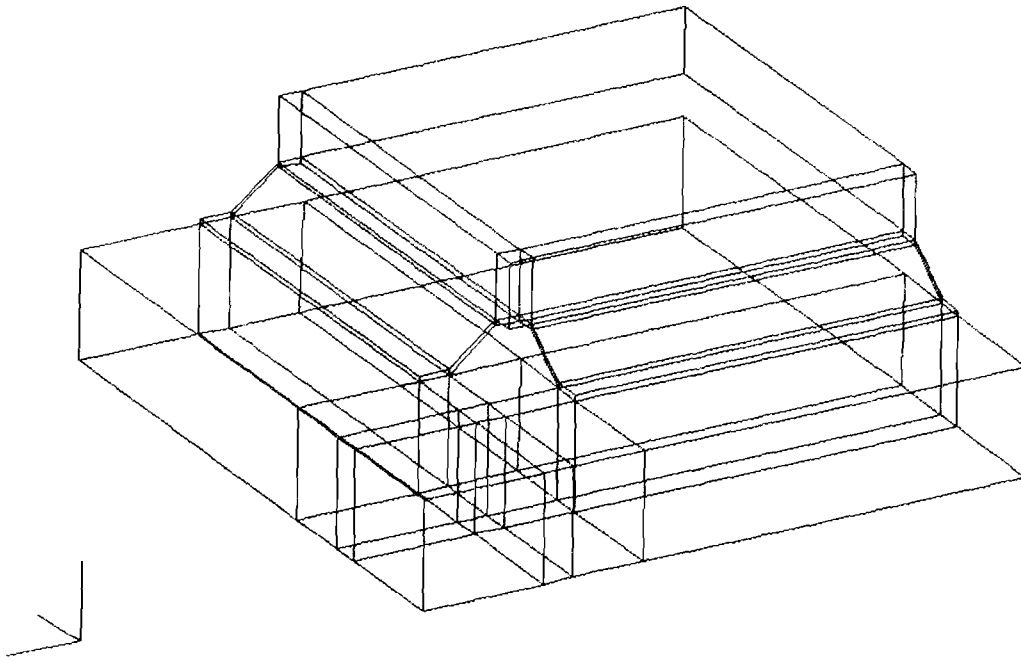


Figure 19: Gull-Wing System Superelement Model

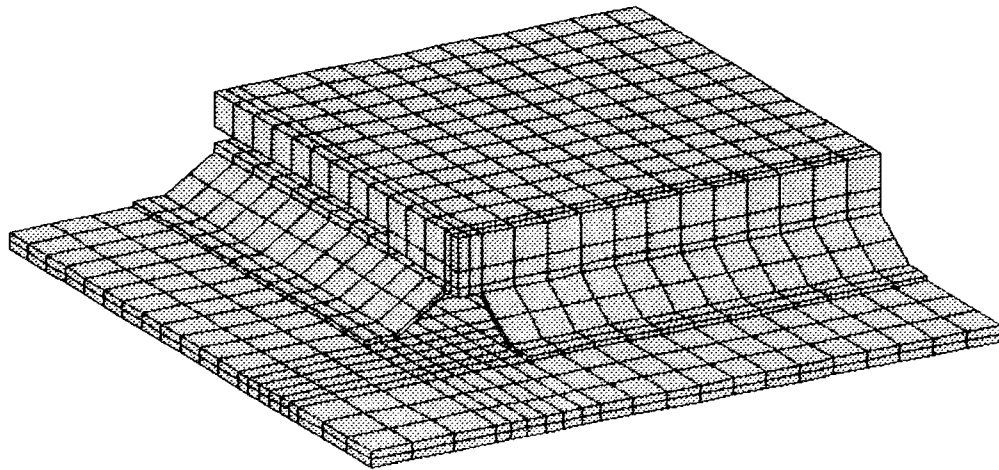


Figure 20: Gull-Wing System FEM

4.1.2 BOARD MODEL

A model representing the eight board layers was generated (Figure 21). This model contained node points on its horizontal axis which corresponded to the locations on the board where the leads connected to the board. The dimensions of this model were the same as the largest package, the gull-wing package. A thermal analysis of the board model was simulated and the results were inputted into the system models.

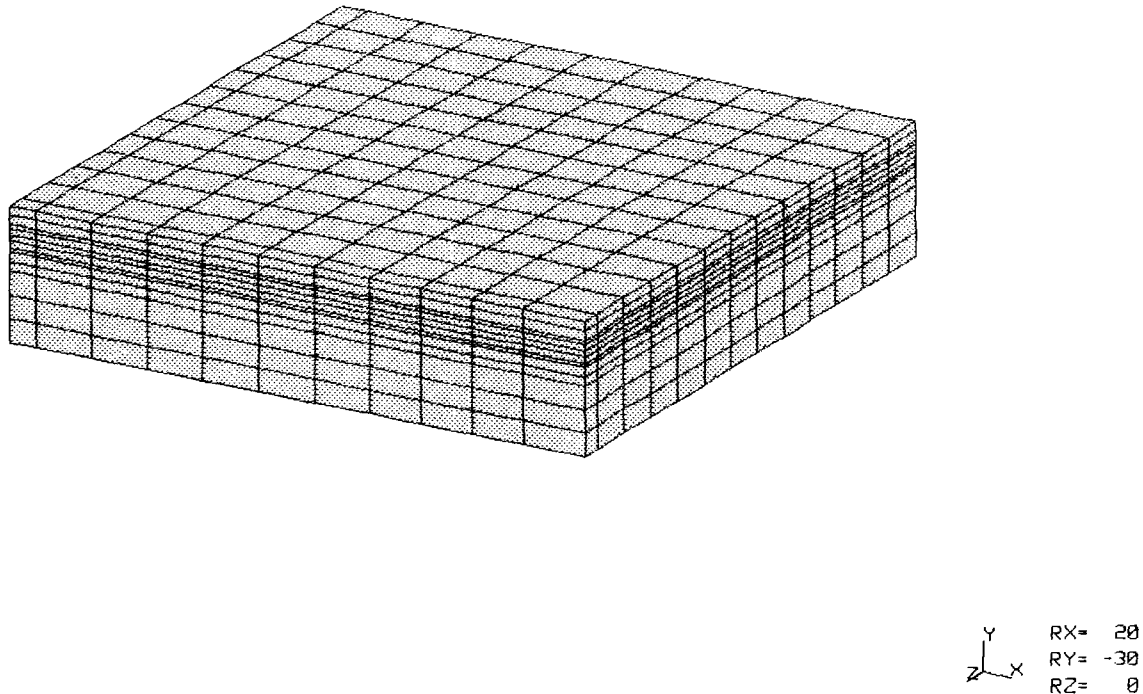


Figure 21: Microwire Board FEM

4.1.3 COMPLIANT CONNECTION MODELS

FEMs were generated for the S-lead, leadless solder joint and gull-wing lead. The leaded models contained the lead and solder elements and

the solder joint model contained only solder elements. Each model has a region representing the lead's contact with the edge of the package and a region representing the lead's contact with the top surface of the board. Deflections from the system models were inputted along these regions and a static analysis simulated. The resulting stress values in the solder were then used to estimate the lead's useful life.

The generation of the S-lead model was straightforward. The entire model was completed in a day. First, a two-dimensional (2-D) model of the lead and the attached solder was created. Eight noded 2-D elements were used in order to obtain the circular geometry, Figure 22a. This model was then extended into the third dimension and 20 noded, 3-D elements were generated, Figure 22b. This model was then meshed and the final model is displayed in Figure 23.

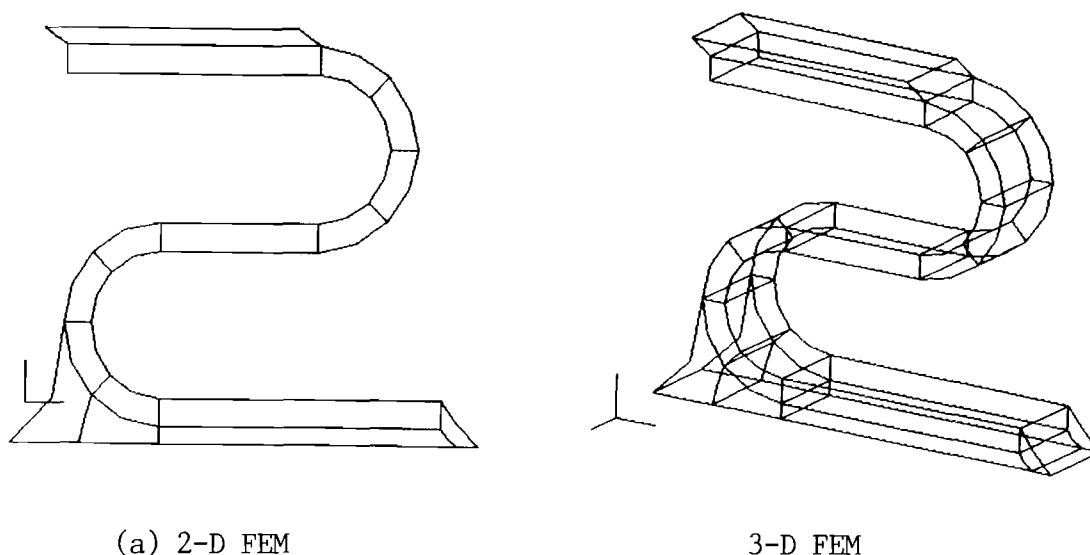


Figure 22: S-Lead Superelement Model

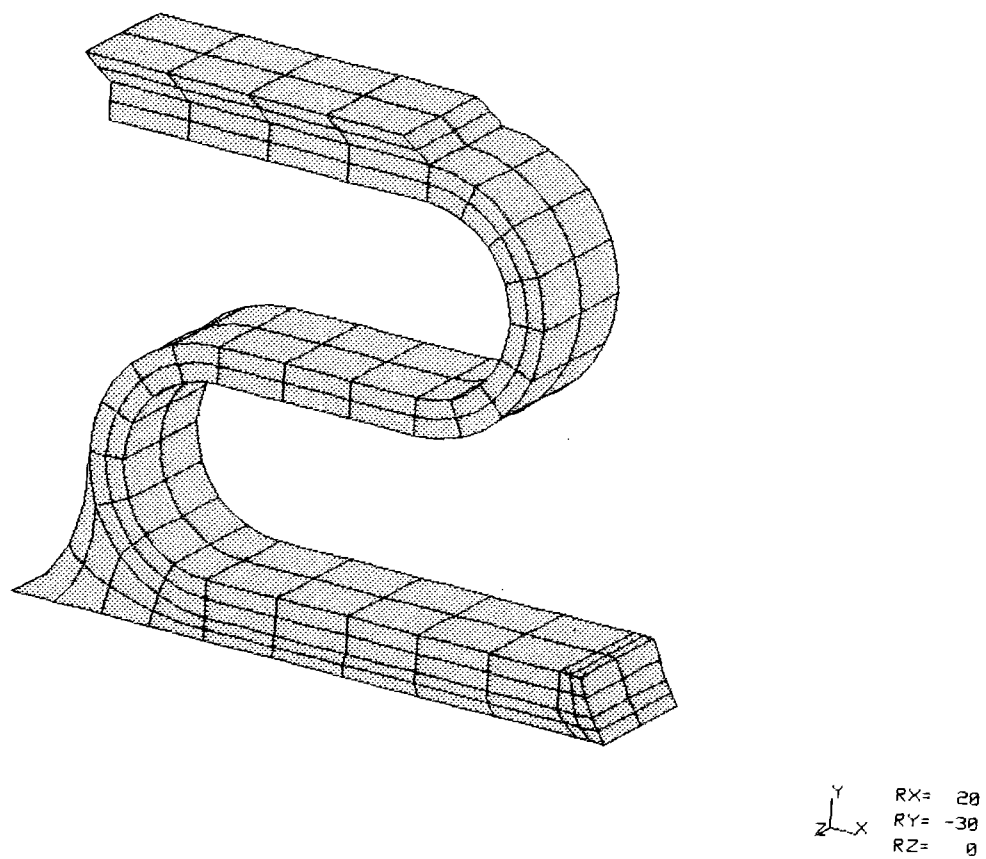


Figure 23: S-Lead FEM

The generation of the leadless solder joint was a more complex process. This model took approximately two weeks to complete. Drawings representing the x-y, x-z and y-z planes were used as guides in the generation process, Figures 24, 25, and 26. This model represents a joint used on a package with 50 mil spacing between joints. The package has castellations and, therefore, the solder curves into the package. The segment representing the solder base was simple to generate since the x-z plane is uniform in the y-direction. The fillet element, however, had to be inputted individually since these elements vary in all three dimensions. The base elements were meshed and then the fillet nodes and elements were defined. The resulting model is shown in Figure 27.

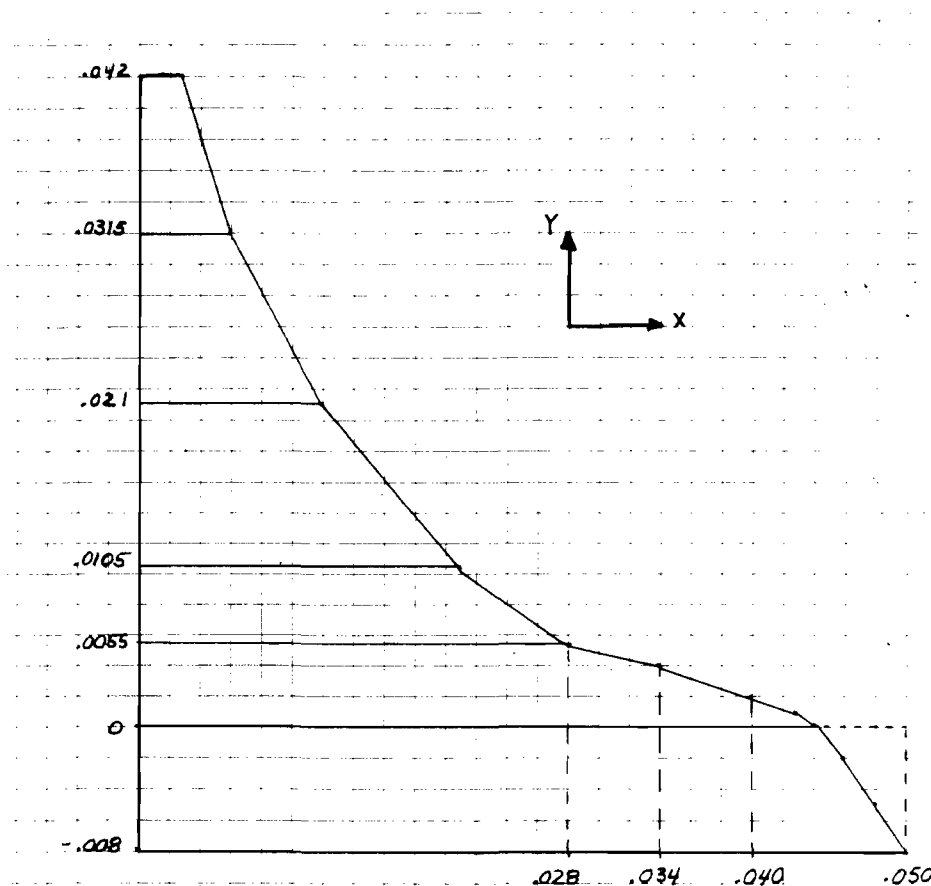


Figure 24: Solder Joint: X-Y Plane

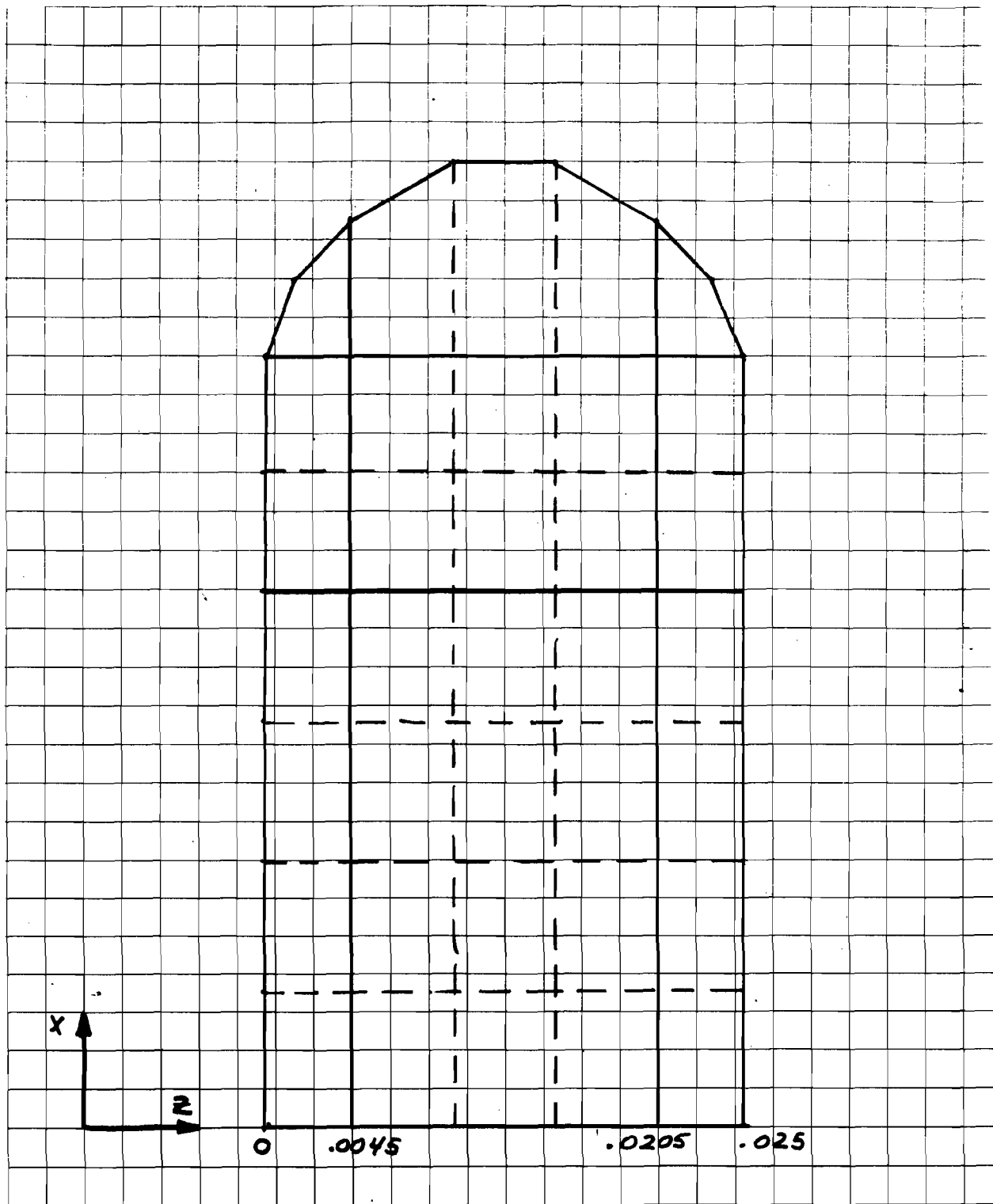


Figure 25: Solder Joint: X-Z Plane

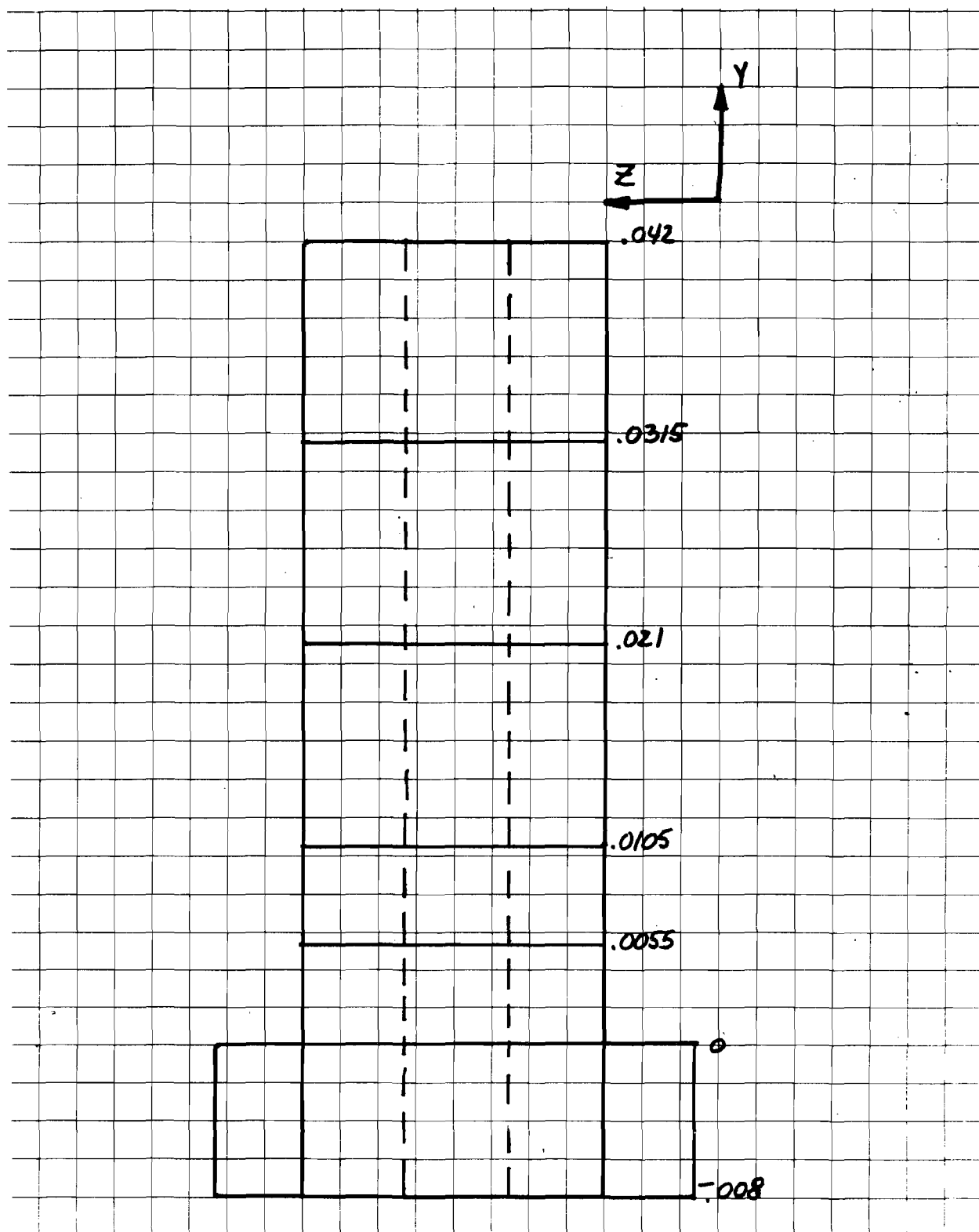


Figure 26: Solder Joint: Y-Z Plane

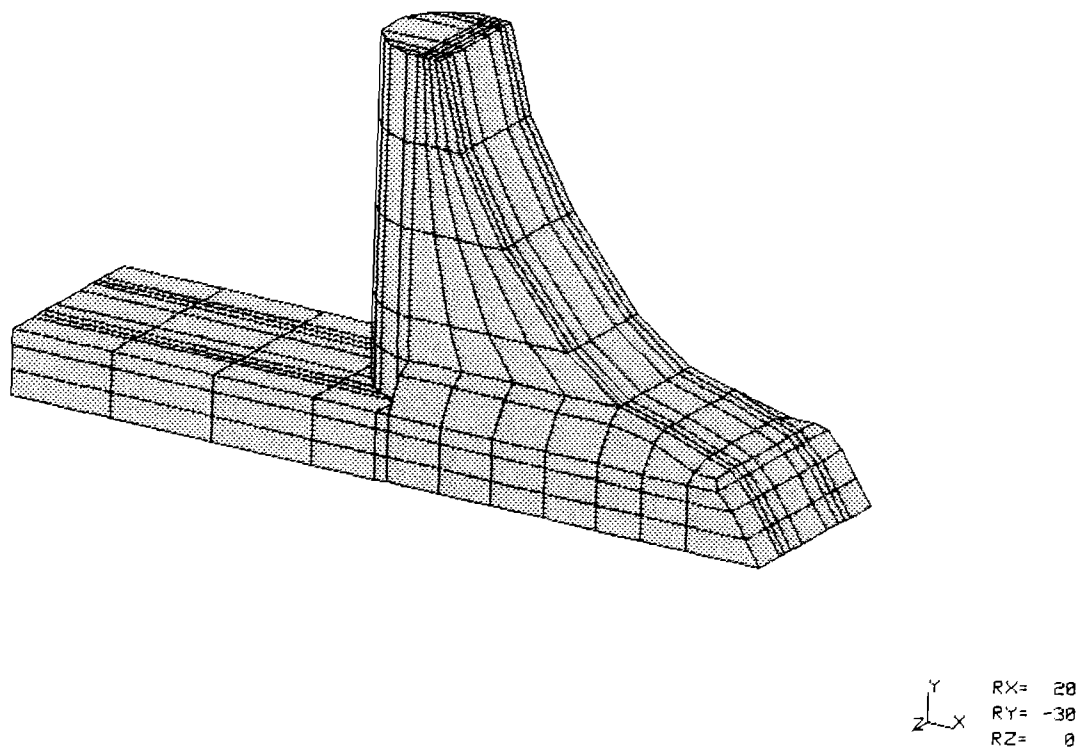


Figure 27: Leadless FEM

The gull-wing model was also simple to generate. A 2-D model was created using eight noded elements representing the solder, lead and brazing materials, Figure 28a. This model was then extended into the third dimension and 20 noded elements were generated. This model was then meshed, Figure 28b. A segment of the lead had to be extended in the z-direction before the final model was completed, Figure 29.

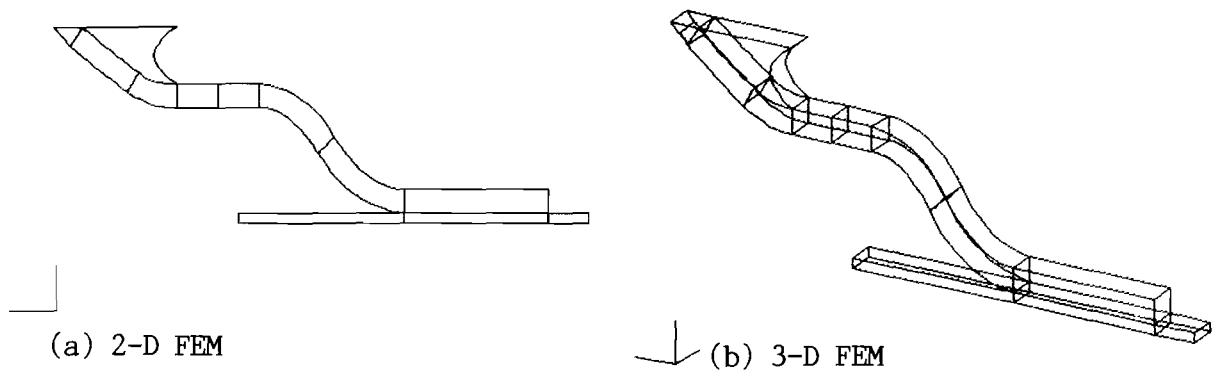


Figure 28: Gull-Wing Superelement Model

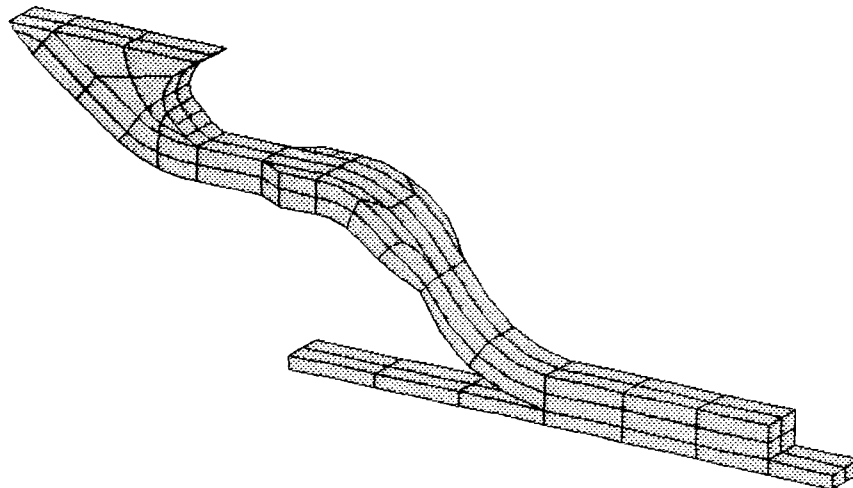


Figure 29: Gull-Wing FEM

4.2 MODELING OF COMPLEX CIRCULAR GEOMETRIES

When generating a FEM, the analysis will create a superelement model outlining the general shape of the system. Normally the different elements in the system will be of the same shape, i.e. circular, rectangular, triangular, etc. In the system that was analyzed, however, there were not only circular geometries embedded within rectangular geometries, but also circular geometries intersecting with other circular geometries. Instead of attempting to use a combination of rectangular and circular elements, only quadrilateral elements were used. Because these elements have corner and midside nodes, rectangular and circular geometries can be defined.

It was obvious that the creation of this model would be complex and take a considerable amount of time. Therefore, preliminary models were created in order to check for round-off error problems in the approach used. The first model created was a wire within a block (Figure 30). An analysis was simulated and no problems occurred. This model was then meshed in all three directions and elements were removed from the center area (Figure 31). Once again, the simulation indicated no problems with this basic design. From this model, it was obvious that only one quarter of the system would need to be modeled for the ideal case where the wire passed directly through the center of the hole. Generation of the actual model now begins.

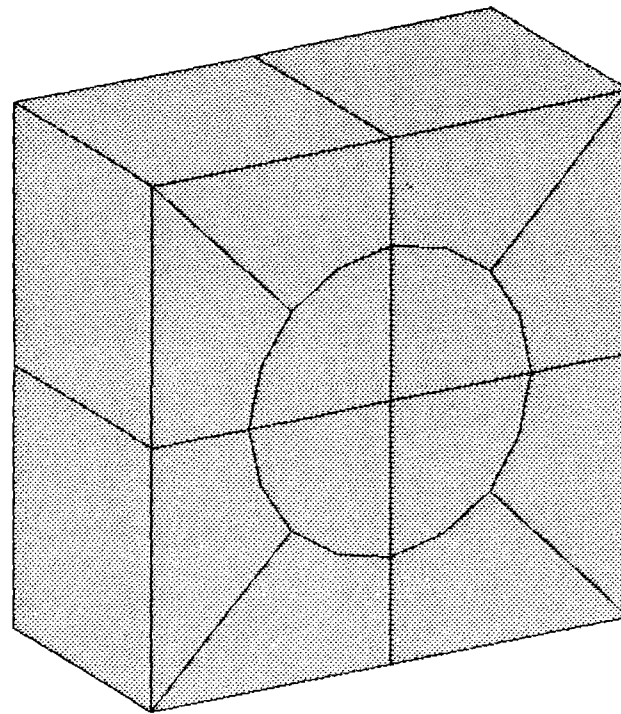


Figure 30: Wire Within A Block

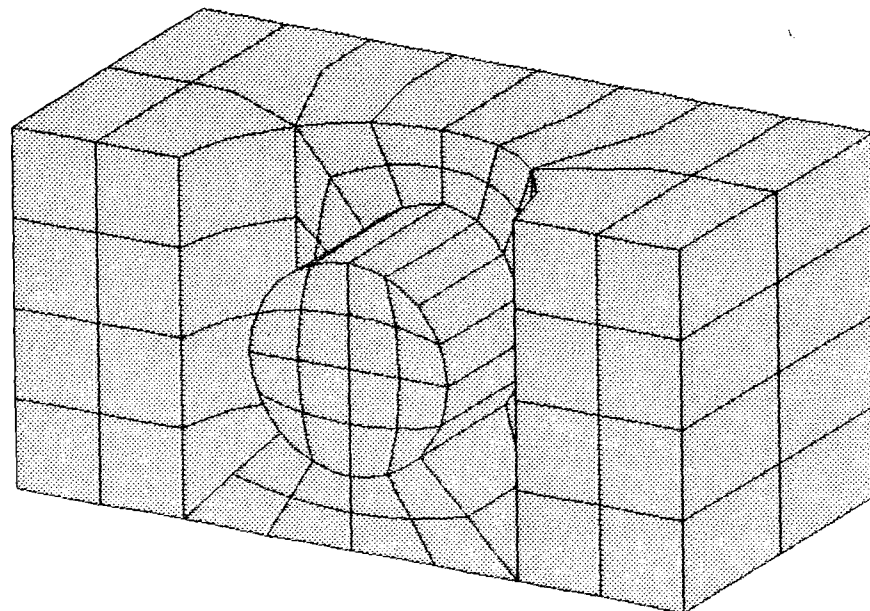
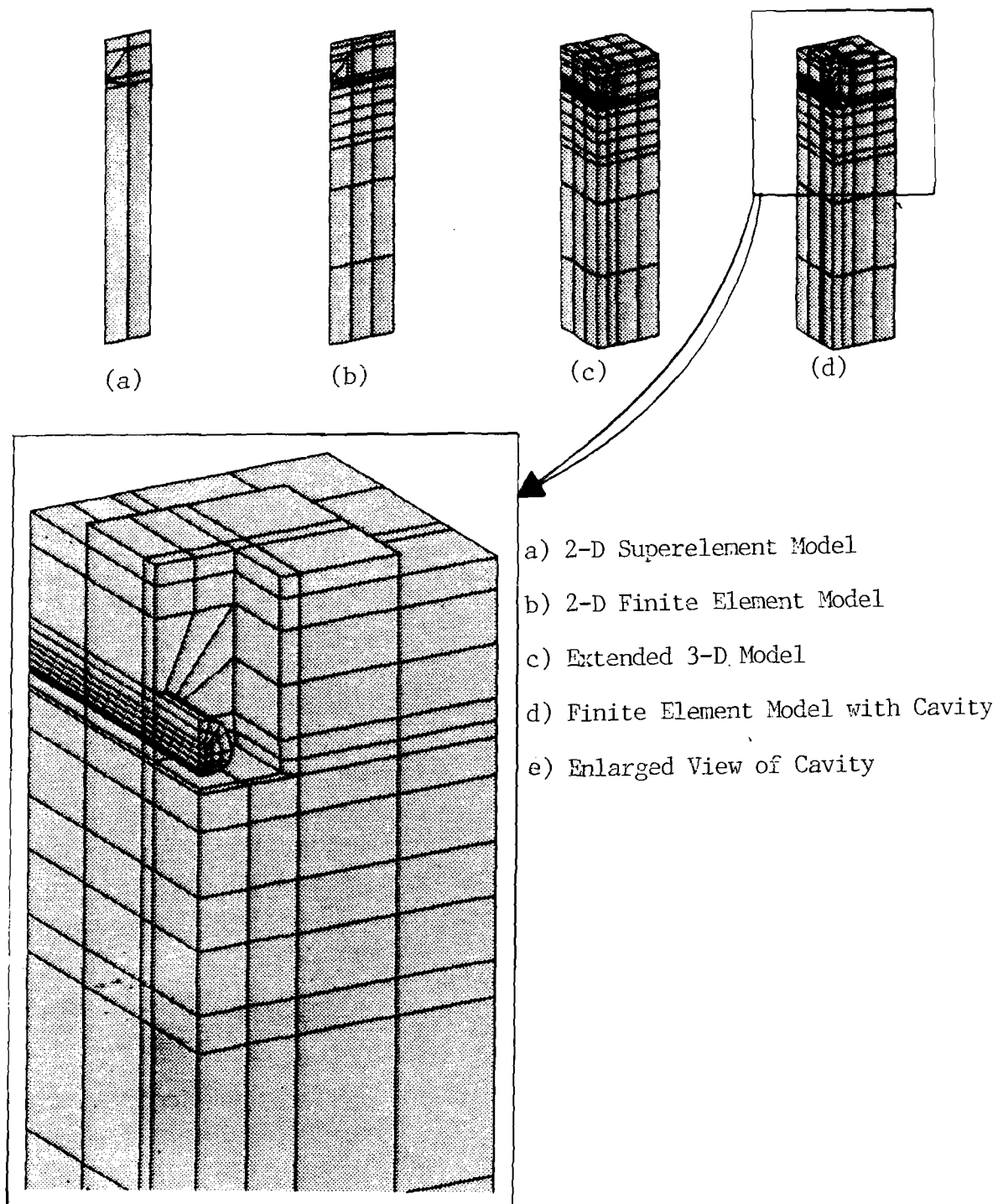


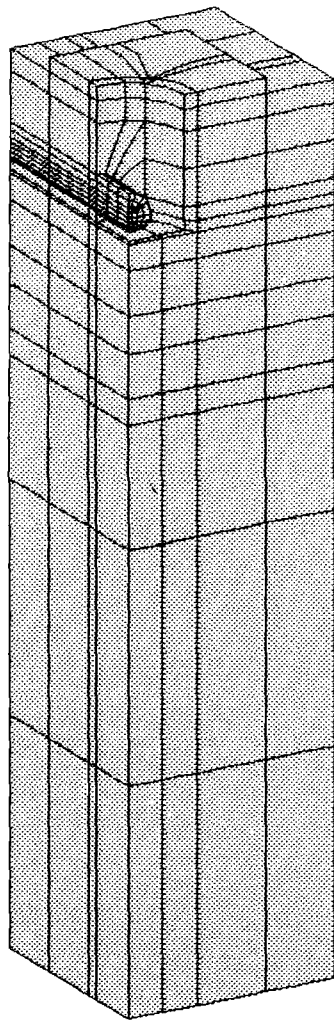
Figure 31: Meshed Block

Using the proper dimensions for the system, another 2-D superelement model using eight noded elements was created (Figure 32a). This model was meshed and a finer model generated (Figure 32b). This finer model was then extended back into the third dimension and 20 noded elements were generated. This model was then meshed (Figure 32c) and the materials were properly identified for all the elements. Two sections had to be removed. The first represented the air elements surrounding the top of the plating and the second represented the air elements within the PTH (Figure 32d). Figure 32e displays an enlarged view of the cavity section. The nodes along the cavity surface were reshaped into a circular hole (Figure 33). Since this surface contained corner and midside nodes, it was necessary to change the location of both sets of nodes. When reshaping a surface such as this one, it is important to be sure that new surfaces do not overlap any existing surfaces.

When the analysis of this was simulated, some round-off errors occurred. This was due to improper meshing by the preprocessor program and was easily corrected by altering the location of specific nodes. The corrected analysis showed that the restraining core elements restrained the board so well that zero deflection could be considered along the top of this surface. The restraining core and the elements below it were eliminated and the board material was expanded in both horizontal directions. Once these elements were expanded, the location of the midside nodes had to be altered to correspond to the new dimensions. Figure 34 shows the FEM for the 20 mil via, PTH. This model was modified to represent a 10 mil via, PTH. The 10 mil via FEM is displayed in Figure 35. The second model was



(e) Figure 32: Microwire/PTH FEM Generation



Y
X
Z
RX= 20
RY= 30
RZ= 0

Figure 33: Microwire/PTH FEM

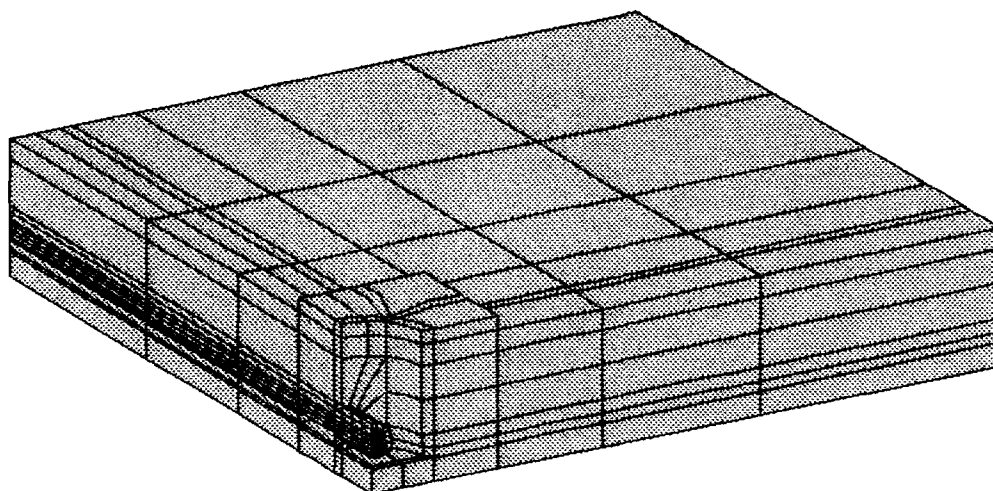


Figure 34: Modified Microwire/PTH FEM (20 Mil Via)

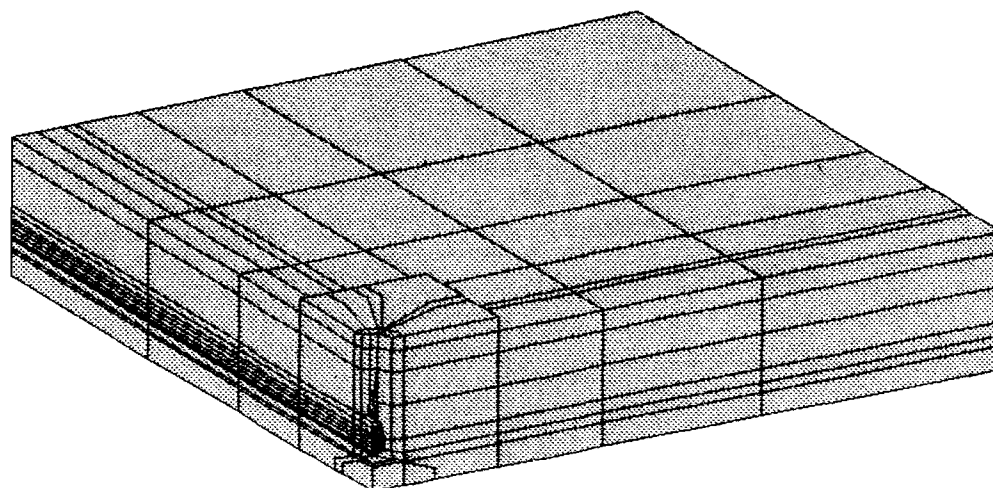


Figure 35: Modified Microwire/PTH FEM (10 Mil Via)

analyzed and the results were used to estimate a useful life of the micro-wire interface connection.

4.3 LESSONS LEARNED

After completing a FEA, it is important to check the results to see if any other simplifications are possible. This information can then be utilized in the future generation of FEM. Two observations were made in regard to this study.

The first observation concerned the package/board/lead system models. The resulting deflections from the three system models showed that the lead design had a negligible effect on the expansion of the package and the board. This indicates that a more complex system model is unnecessary. Only a FEM of the package and a FEM of the board would be generated and two separate analyses on the model performed. Since both the package and the board are rectangular in shape, generation of these models would be extremely simple. In addition, a single model could be generated to represent several different package and board sizes. The resulting deflections along different locations could be inputted into the individual lead models. An assessment of the effect package size has on the estimated life could be made.

The second observation concerned the microwire/PTH interface connection. The results showed that the board material away from the region of concern had negligible stress and that the stresses in the region of

concern had little variance between the two different models. This indicates that a much simpler model representing only a small segment in the area of interest would have been sufficient. This reduction in complexity would also be beneficial in the modeling of a wire that was off center since, in this case, a one-quarter model could not be used and the entire geometry would have to be modeled.

5.0 TRANSFER OF FINITE ELEMENT RESULTS

When stress caused by a static load is a concern, the engineer performs a finite element analysis and compares the resulting stresses to the yield stresses for the different materials. What can be done when the load is not static, but varies with time? The specific problem dealt with in this analysis was stresses caused by thermal cycling conditions. These stresses eventually resulted in fatigue of the ductile materials. A technique was needed to transfer the results of the FEA to a value of merit which could be used to assess the reliability of the design.

The method used followed a simple procedure. First, a FEM was generated. Static analyses were simulated for the temperature change of stress free temperature to maximum temperature (high temperature cycle) and for the temperature change of stress free temperature to minimum temperature (low temperature cycle). The resulting maximum Von-Mises stress value for the material of concern was obtained. In this study, the two materials of concern were the ductile materials, copper and solder. The strain range for this cyclic condition was calculated by adding the individual strains for the low temperature and the high temperature cycles. These strains had to include both the elastic strain and the plastic strain. Since the exact plastic strain could not be determined without performing a nonlinear analysis, a range for this strain was determined and it was assumed that the actual plastic strain was in between these two values (see section 3.0 for a more detailed explanation).

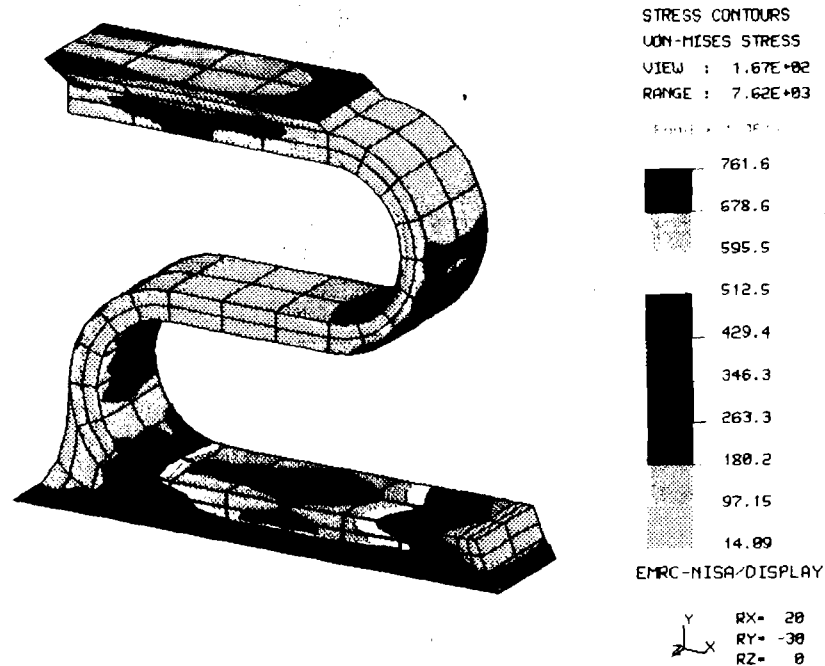
Once the strain range value was obtained, this value was plotted onto a curve representing the strain range versus the number of cycles to failure for the particular temperature range that was used (minimum temperature to maximum temperature). This curve was generated from the Coffin-Manson equation as described in section 3.0. Two values of cycles to failure were obtained for each analysis. One presented the low plastic strain and the other the high plastic strain. The resulting range of the number of thermal cycles to failure gave an indication of the useful life of the component. This procedure will now be applied to the FEM developed in section 4.0.

5.1 S-LEAD CONNECTION

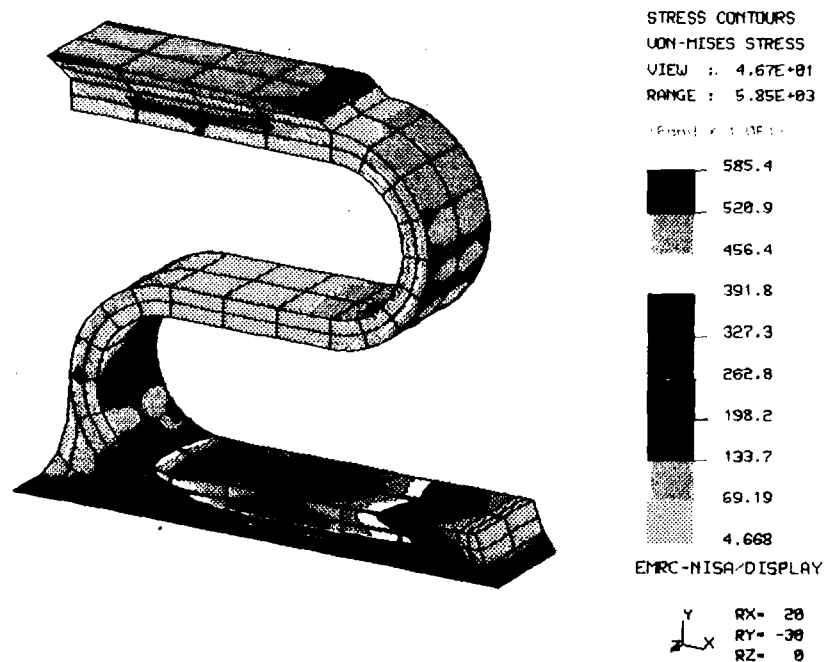
The high and low temperature cycle Von-Mises stress contours in the S-lead connection are displayed in Figure 36. The overall maximum stress does not occur in the solder material, but in the lead material. This stress value is well below the yield point for the lead material. The solder's maximum linear stress and plastic stress are:

<u>SIMULATION</u>	<u>MAXIMUM LINEAR STRESS</u>	<u>PLASTIC STRESS</u>
High Temp Cycle	6,000 psi	2,800 psi
Low Temp Cycle	3,900 psi	700 psi

The elastic strain is .0029 in/in (3,200 psi/1,090,000 psi). The estimated plastic strain and the total strain are:



(a) Low Temperature Cycle



(b) High Temperature Cycle

Figure 36: Stress Contours for S-Lead FEM

High Temperature Cycle

<u>METHOD</u>	<u>PLASTIC STRAIN</u>	<u>TOTAL STRAIN</u>
1	$2,800/1.09 \times 10^6 = .0026 \text{ in/in}$	$.0029 + .0026 = .0055 \text{ in/in}$
2	$.0026 \times 2 = .0052 \text{ in/in}$	$.0029 + .0052 = .0081 \text{ in/in}$

Low Temperature Cycle

<u>METHOD</u>	<u>PLASTIC STRAIN</u>	<u>TOTAL STRAIN</u>
1	$700/1.09 \times 10^6 = .0006 \text{ in/in}$	$.0029 + .0006 = .0035 \text{ in/in}$
2	$.0006 \times 2 = .0012 \text{ in/in}$	$.0029 + .0012 = .0041 \text{ in/in}$

The overall total strain for high and low temperature cycles for the S-lead connection is:

Method 1	$.0055 + .0035 = .0090 \text{ in/in}$
Method 2	$.0081 + .0041 = .0122 \text{ in/in}$

These overall strain values were plotted on the elastic plus plastic line of the Coffin-Manson curve for solder (Figure 11) and the following number of cycles to failure range was obtained: 11,500 to 60,000 cycles.

5.2 LEADLESS CONNECTION

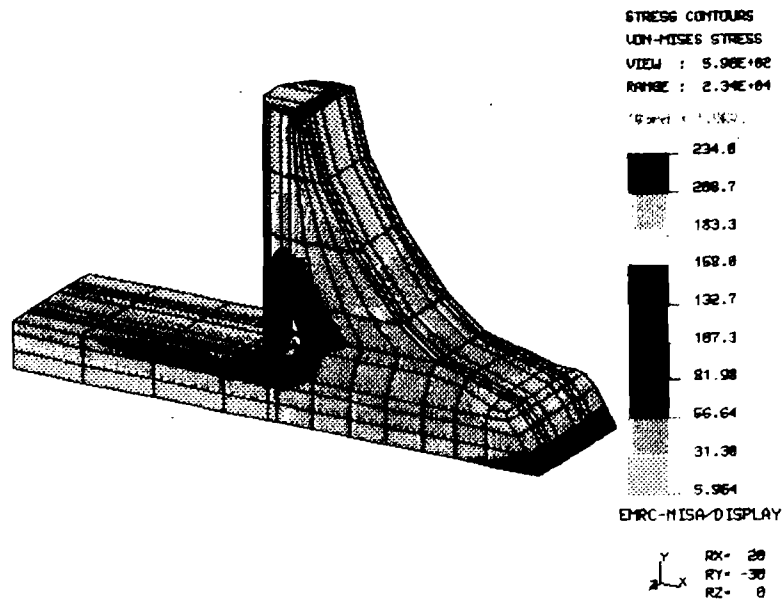
The leadless solder connection model consists entirely of solder elements. Figure 37 displays the high and low temperature cycle Von-Mises stress contours for this analysis. The solder's maximum linear stress and plastic stress are:

<u>SIMULATION</u>	<u>MAXIMUM LINEAR STRESS</u>	<u>PLASTIC STRESS</u>
High Temp Cycle	23,400 psi	20,200 psi
Low Temp Cycle	7,698 psi	4,498 psi

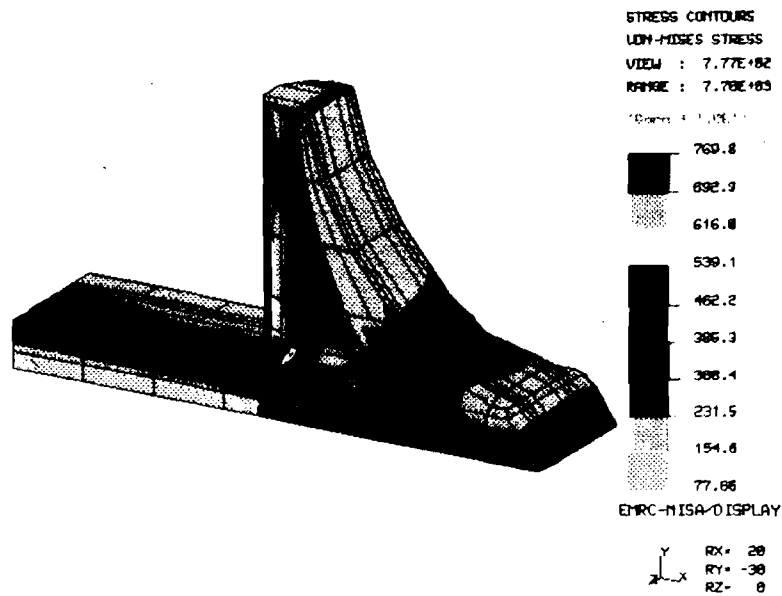
These values are both beyond solder's yield stress of 3,200 psi. The elastic strain is .0029 in/in (3,200 psi/1,090,000 psi). The estimated plastic strain and the total strain are:

High Temperature Cycle

<u>METHOD</u>	<u>PLASTIC STRAIN</u>	<u>TOTAL STRAIN</u>
1	$20,200 / 1.09 \times 10^6 = .0185 \text{ in/in}$	$.0029 + .0185 = .0214 \text{ in/in}$
2	$.0185 \times 2 = .0370 \text{ in/in}$	$.0029 + .0370 = .0399 \text{ in/in}$



(a) Low Temperature Cycle



(b) High Temperature Cycle

Figure 37: Stress Contours for Leadless FEM

Low Temperature Cycle

<u>METHOD</u>	<u>PLASTIC STRAIN</u>	<u>TOTAL STRAIN</u>
1	$4,498 / 1.09 \times 10^6 = .0041 \text{ in/in}$	$.0029 + .0041 = .0070 \text{ in/in}$
2	$.0041 \times 2 = .0082 \text{ in/in}$	$.0029 + .0082 = .0111 \text{ in/in}$

The overall total strain for high and low temperature cycles for the S-lead connection is:

Method 1 $.0214 + .0070 = .0284 \text{ in/in}$

Method 2 $.0399 + .0111 = .0510 \text{ in/in}$

These overall strain values were plotted on the elastic plus plastic line of the Coffin-Manson curve for solder (Figure 11) and the following number of cycles to failure range was obtained: 120 to 260 cycles.

5.3 GULL-WING CONNECTION

The high and low temperature cycle Von-Mises stress contours in the gull-wing connection are displayed in Figure 38. Once again, the overall maximum linear stress does not occur in the solder, but in the lead material and this stress value is well below the yield point for this material. The solder's maximum stress and plastic stress are:

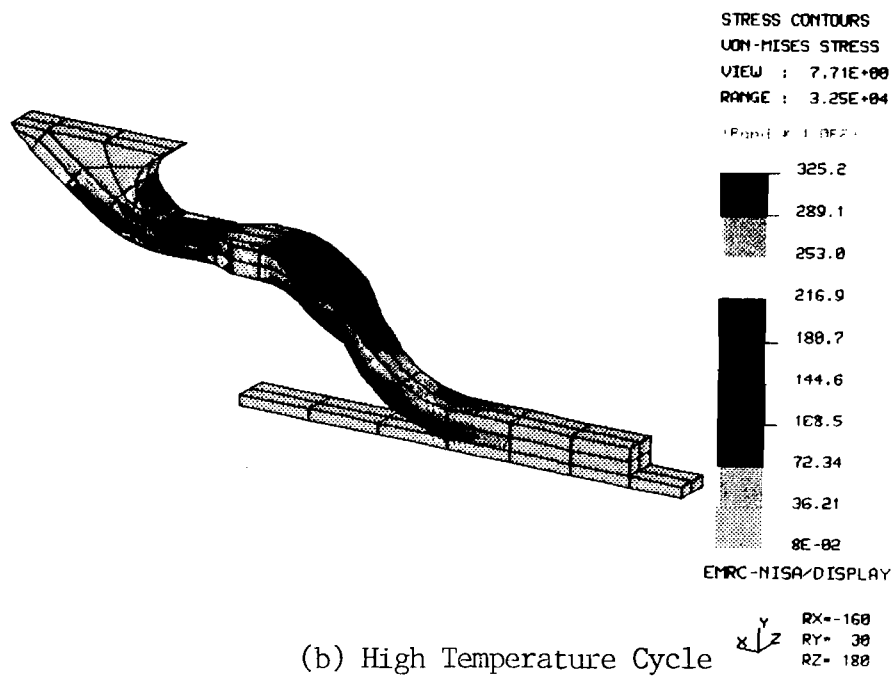
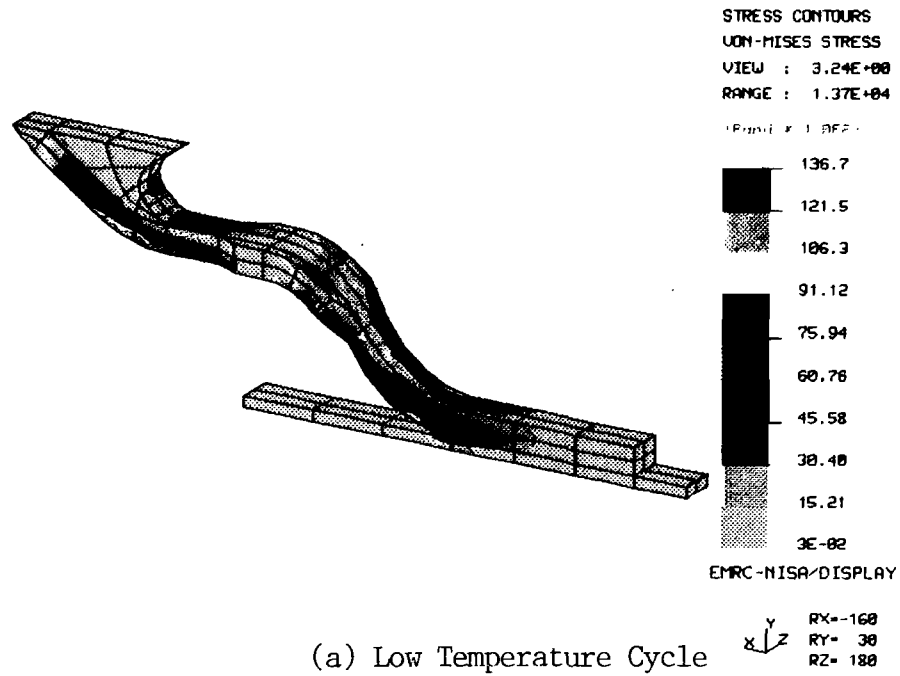


Figure 38: Stress Contours for Gull-Wing FEM

<u>SIMULATION</u>	<u>MAXIMUM LINEAR STRESS</u>	<u>PLASTIC STRESS</u>
High Temp Cycle	2,700 psi	-----
Low Temp Cycle	4,250 psi	1,050 psi

Only the low temperature cycle value is beyond solder's yield stress of 3,200 psi. The elastic strain, the estimated plastic strain, and the total strain are:

High Temperature Cycle

The elastic strain is .0025 in/in (2,700 psi/1,090,000 psi). Since there is no plastic strain, then the total strain is .0025 in/in.

Low Temperature Cycle

The elastic strain is .0029 in/in (3,200 psi/1,090,000 psi).

<u>METHOD</u>	<u>PLASTIC STRAIN</u>	<u>TOTAL STRAIN</u>
1	$1,050/1.09 \times 10^6 = .0010 \text{ in/in}$	$.0029 + .0010 = .0039 \text{ in/in}$
2	$.0010 \times 2 = .0020 \text{ in/in}$	$.0029 + .0020 = .0049 \text{ in/in}$

The overall total strain for high and low temperature cycles for the gull-wing connection is:

Method 1 $.0025 + .0039 = .0064$ in/in

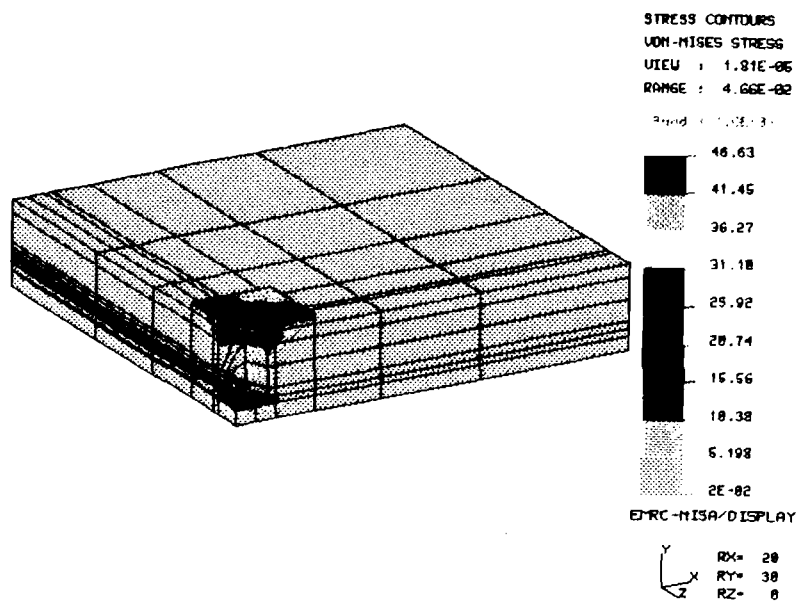
Method 2 $.0025 + .0049 = .0074$ in/in

These overall strain values were plotted on the Coffin-Manson curve for solder (Figure 11) and the following number of cycles to failure range was obtained: 400,000 to 2,000,000 cycles.

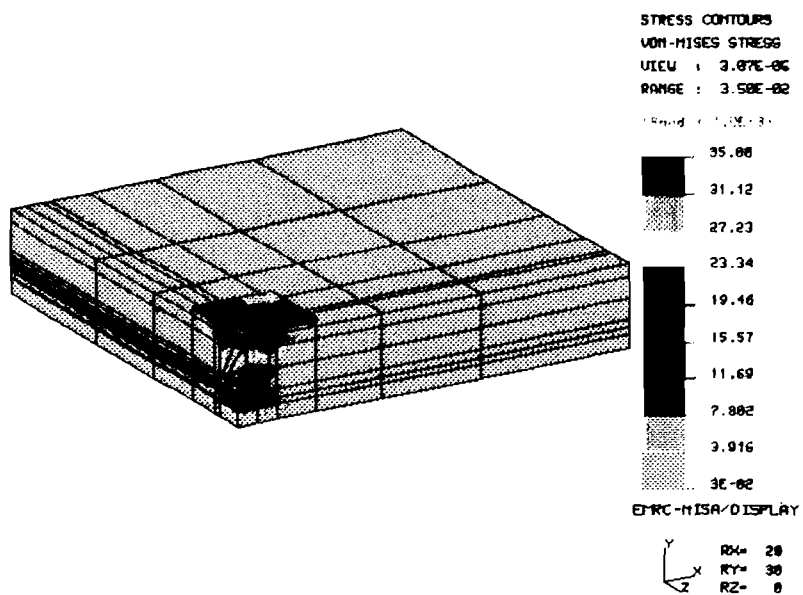
5.4 MICROWIRE/PTH CONNECTION

Four analyses were performed on the two connection models. Figure 39 displays the Von-Mises Stress contours for the 20 mil via model and Figure 40 displays the contours for the 10 mil via model. The majority of the board has very little stress with the high stresses occurring in the plated copper and the copper microwire. The highest stresses occurred at the plated barrel where the pad contacts the board. These values were not used in this analysis because that area was not the area of reliability concern. The maximum linear stress found in the copper wire/PTH interface is listed below for the four different analyses.

<u>SIMULATION</u>	<u>LINEAR STRESS</u>	<u>PLASTIC STRESS</u>
10 Mil Via, High Temp Cycle	19,000 psi	11,000 psi
10 Mil Via, Low Temp Cycle	19,000 psi	11,000 psi
20 Mil Via, High Temp Cycle	10,000 psi	2,000 psi
20 Mil Via, Low Temp Cycle	8,000 psi	0 psi

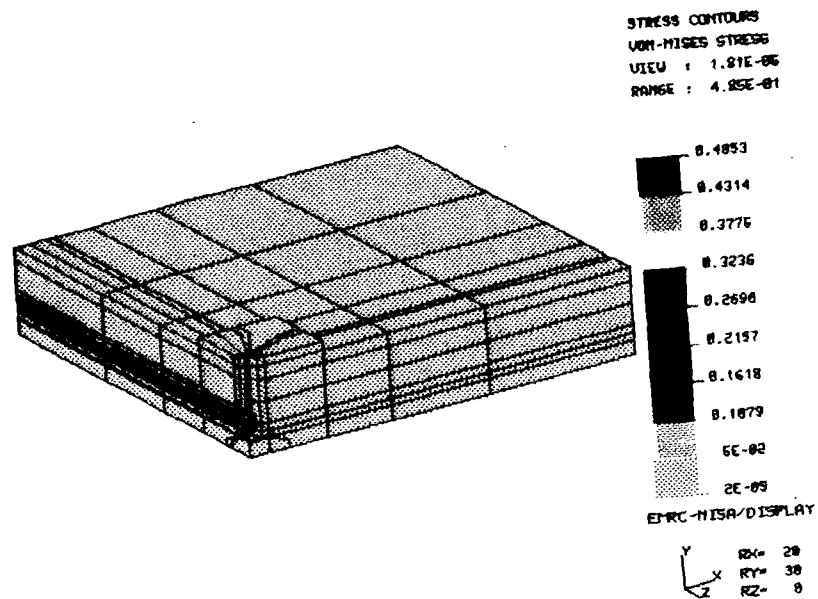


(a) Low Temperature Cycle

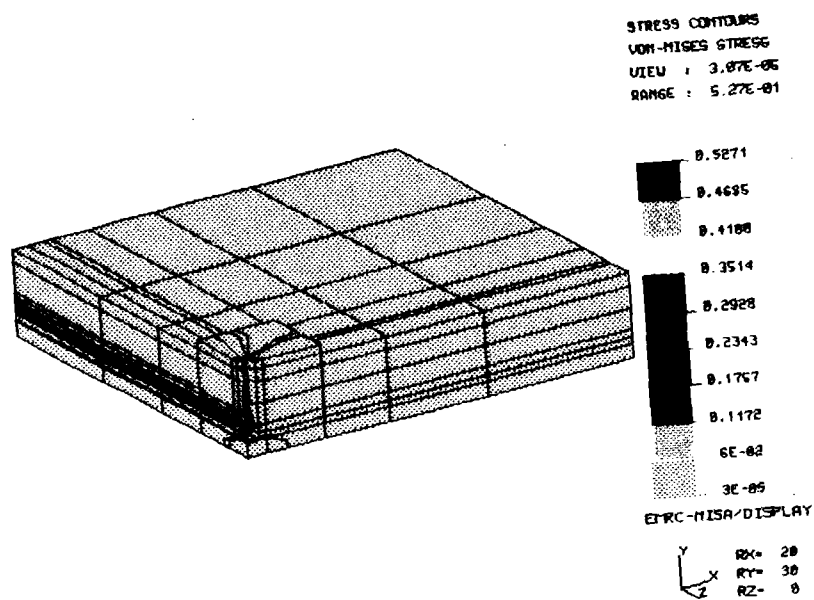


(b) High Temperature Cycle

Figure 39: Stress Contours for Microwire/PTH (20 Mil Via)FEM



(a) Low Temperature Cycle



(b) High Temperature Cycle

Figure 40: Stress Contours for Microwire/PTH (10 Mil Via) FEM

Since the elastic limit for copper is 8,000 psi and each simulation met or exceeded this value, the elastic strain is the elastic stress divided by the modulus of elasticity, which comes to .0005 in/in ($8,000\text{psi}/16,000,000\text{psi}$). The estimated plastic stress is then the difference between the maximum linear stress and the yield stress as shown above. The estimated plastic strain and the total strain are calculated below:

10 Mil Via, High Temperature Cycle

<u>METHOD</u>	<u>PLASTIC STRAIN</u>	<u>TOTAL STRAIN</u>
1	$11,000/16 \times 10^6 = .0007 \text{ in/in}$	$.0005 + .0007 = .0012 \text{ in/in}$
2	$2 \times .0007 = .0014 \text{ in/in}$	$.0005 + .0014 = .0019 \text{ in/in}$

10 Mil Via, Low Temperature Cycle

<u>METHOD</u>	<u>PLASTIC STRAIN</u>	<u>TOTAL STRAIN</u>
1	$11,000/16 \times 10^6 = .0007 \text{ in/in}$	$.0005 + .0007 = .0012 \text{ in/in}$
2	$2 \times .0007 = .0014 \text{ in/in}$	$.0005 + .0014 = .0019 \text{ in/in}$

The overall total strain for high and low temperature cycles for the 10 mil via is:

<u>METHOD</u>	<u>OVERALL STRAIN</u>
1	.0012 + .0012 = .0024 in/in
2	.0019 + .0019 = .0038 in/in

20 Mil Via, High Temperature Cycle

<u>METHOD</u>	<u>PLASTIC STRAIN</u>	<u>TOTAL STRAIN</u>
1	$2,000/16 \times 10^6 = .0001 \text{ in/in}$.0005 + .0001 = .0006 in/in
2	$2 \times .0001 = .0002 \text{ in/in}$.0005 + .0002 = .0007 in/in

20 Mil Via, Low Temperature Cycle

<u>METHOD</u>	<u>PLASTIC STRAIN</u>	<u>TOTAL STRAIN</u>
1	0 in/in *	.0005 + 0 = .0005 in/in
2	0 in/in *	.0005 + 0 = .0005 in/in

*Note: The Von-Mises stress value did not exceed the elastic limit, therefore, there was no plastic strain.

The overall total strain for the high and low temperature cycles for the 20 mil via is:

<u>METHOD</u>	<u>OVERALL STRAIN</u>
1	$.0006 + .0005 = .0011 \text{ in/in}$
2	$.0007 + .0005 = .0012 \text{ in/in}$

These overall strain values were plotted on the plastic plus elastic Coffin-Manson curve for copper (Figure 11) and the following number of cycles to failures ranges were obtained:

10 mil via: 110,000 to 10,000,000
20 mil via: greater than or equal to 10,000,000

6.0 CONCLUSIONS

Several Finite Element Analyses (FEA) were performed and the results used to estimate the useful life of the various connections. For the surface mounted lead connections, the results indicated that the leadless connections would only survive a minimal number of thermal cycles before problems occurred (less than 260 cycles). The S-lead and gull-wing leads, however, showed very good survival rates. It was estimated that the S-lead would survive between 11,500 and 60,000 thermal cycles and that the gull-wing lead would survive between 600,000 and 2,000,000 thermal cycles. This indicates that the two leaded designs will have superior reliability performance.

The results from the analysis on the microwire and Plated-Through-Hole (PTH) connection indicate that, under ideal conditions, this connection will survive a minimum of 110,000 thermal cycles. These results must be carefully considered. Due to insufficient information and time, an analysis of nonideal configurations was not performed. There are two types of microwire connections that would be of serious reliability concern. The first type is where the wire does not pass straight through the PTH (180 degrees), but is rotated at an angle (135 or 90 degrees). The second type of connection is where the microwire is allowed the maximum variation from the ideal condition. An analysis under these conditions would predict the reliability of the worst acceptable microwire connection.

In addition to the reliability assessments, conclusions can be made about the finite element modeling and how this process can be improved. Listed below are four observations that have been identified:

1. The results of the FEA on the microwire connection indicate that a much smaller, less-refined model might have been sufficient to analyze this connection. This alternate model would have reduced the model generation time by at least 50 percent and would have provided the time needed to generate a model of the nonideal case where the wire is off center.

2. The resulting stress values in the center of the microwire in the microwire connection FEM were not as harmonious with one another as these values should have been. This indicates that instead of using quadralateral elements only and distorting some of the elements to a considerable degree, a mixing of element types would be preferential. In this case, the quadralateral elements were so distorted in the center of the microwire that the elements took on the approximate shape of a triangle. This would explain the inconsistency of stress values. Instead, these center elements should have been triangles.

3. In the FEMs of the individual leads, the deflections across the width of the leads (25 mils) were essentially constant. These results indicated that the leads could have been modeled in two dimensions versus three dimensions.

4. A comparison of the FEA results for the three different package/board/lead models showed only a slight variation in package and board deflections for the three models. This occurrence implies that the lead type has little effect on the package and board deflections. Consequently, a single package FEM and a single board FEM could be generated and used for the analysis of many different lead types.

The work documented in this report is just a stepping stone in the development of a method to transfer FEA results to a useful estimate of reliability. There are several areas in this analysis, in both the finite element modeling and the transfer of results, that deserve further investigation. Two of these areas are outlined below:

1. The validity of performing a purely linear, elastic analysis and using the results to estimate the amount of plastic strain should be verified. A question arises as to the ability to predict the response of the material once it goes beyond the linear range. There is some indication that, in fact, a nonlinear, elastic and plastic analysis should be performed instead.

2. If these connection models could be significantly simplified, a full-view model, rather than a one-quarter model, could be generated without exceeding the computer's limit. The full-view model would then be used to perform a vibration analysis.

7.0 REFERENCES

1. Sandor, Bela I., "Fundamentals of Cyclic Stress and Strain", The University of Wisconsin Press, 1972.
2. Bivens, Gretchen A. and Bocchi, William J., "Reliability Analysis of a Surface Mounted Package Using Finite Element Simulation", October, 1987, RADC-TR-87-177.
3. Bivens, Gretchen A., "Reliability Assessment of Surface Mount Technology (SMT)", March, 1988, RADC-TR-88-72.



MISSION of Rome Air Development Center

RADC plans and executes research, development, test and selected acquisition programs in support of Command, Control, Communications and Intelligence (C³I) activities. Technical and engineering support within areas of competence is provided to ESD Program Offices (POs) and other ESD elements to perform effective acquisition of C³I systems. The areas of technical competence include communications, command and control, battle management information processing, surveillance sensors, intelligence data collection and handling, solid state sciences, electromagnetics, and propagation, and electronic reliability/maintainability and compatibility.

